ADVANCED FUNCTIONAL MATERIALS
www.afm-journal.de

Recent Progress in Liquid Electrolytes for High-Energy Lithium–Metal Batteries: From Molecular Engineering to Applications

Nan Li, Xue Han, Xinke Cui, Chaohe Xu, Chong Mao,* Xiaobing Dai,* and Weijiang Xue**

Lithium–metal batteries (LMBs) have garnered significant interests for their promising high gravimetric energy density (E_g) ~ 750 Wh kg^{-1}. However, the practical application of the LMBs is plagued by the high reactivity and large volume change during charging–discharging of the lithium–metal anode (LMA), seriously deteriorating the battery safety and cycle life. Great efforts have been devoted to tailoring the electrolytes to favor the Li–metal electroplating by uniformizing the deposition morphology and by suppressing the side reactions between electrolytes and LMA. The aggressive chemistries of both the LMA and its high-voltage counterpart give new electrolyte components more opportunities, especially designing via molecular engineering. Here, a comprehensive and in-depth overview of the scientific challenges, fundamental mechanisms, and particularly historical strategies of designing new molecules for electrolyte components including solvents, salts, and additives. Their important roles in tuning the Li$^+$ solvation structure, interface composition, decomposition pathways, and the resultant electrochemical performance of LMBs are also presented. Finally, novel insights and promising research directions from the practical application viewpoints are proposed for future electrolyte designs for high-voltage LMBs.

1. Introduction

Lithium-ion batteries (LIBs) based on the traditional graphite anode are approaching their gravimetric energy density (E_g) ceiling of ≈300 Wh kg^{-1} with the possibility to reach 400 Wh kg^{-1} level when replacing with SiO/graphite or Si/graphite anodes.[1,2] LIBs can satisfy the requirements for most current applications like electric vehicles (EVs) and energy storage systems (EESs).[3–6] For promising applications in the future like electric Vertical Take-off and Landing (eVTOL) and intelligent robots, however, E_g is required to exceed 500 Wh kg^{-1}. Therefore, it is urging us to seek anode candidates with higher capacity. Due to its high theoretical specific capacity (3860 mAh g^{-1}), low potential (−3.04 V vs standard hydrogen electrode [SHE]), the lithium-metal anode (LMA) is one of the most promising candidates among all anodes and the E_g of lithium-metal batteries (LMBs) can achieve up to a cell-level E_g ~ 750 Wh kg^{-1},[7–12] which significantly inspires the research enthusiasm of scientists from both the academia and the industry (**Figure 1a**).

Unfortunately, the practical application of the LMBs is plagued by the high reactivity and large volume change during charging–discharging of the metallic Li (Li^0), which directly impacts the battery safety and cycle life (Figure 1b). On one hand, almost all organic solvents in electrolytes could not be thermodynamically stable against the LMA. Similar to the graphite anode, the formation of solid electrolyte interphase (SEI), which needs to be Li$^+$ conductive but stop electron tunneling, is required for kinetically stabilizing the Li^0 surface. On the other hand, the morphology of the Li^0 deposition tends to be dendritic, featuring its large surface area consuming both the Li and electrolyte reservoir to form massive SEI. Side reactions between Li^0 and electrolyte are proportional to the Li^0 surface area. The "infinite" volume change upon Li^0 depositing and stripping also induces repeated breaking-formation of the SEI, generating thick and insulating SEI over many cycles. Therefore, such massive and unstable SEI results in low Coulombic efficiency (CE) and sudden cell failure due to the exhaustion of either the active Li reservoir or the

N. Li, X. Cui, W. Xue
Center for Advancing Materials Performance from the Nanoscale
State Key Laboratory for Mechanical Behavior of Materials
Xi'an Jiaotong University
Xi'an 710049, China
E-mail: xuewj@xjtu.edu.cn

X. Han
State Key Laboratory of Metal Matrix Composites
Shanghai Jiao Tong University
Shanghai 200240, China

C. Xu
College of Materials Science and Engineering
Chongqing University
Chongqing 400044, China
E-mail: xche@cqu.edu.cn

C. Mao, X. Dai
Zhuhai Smoothway Electronic Materials Co., Ltd
Zhuhai 519100, China
E-mail: cmao@sw-zh.com; xbdai@sw-zh.com

The ORCID identification number(s) for the author(s) of this article can be found under https://doi.org/10.1002/adfm.202409431

DOI: 10.1002/adfm.202409431

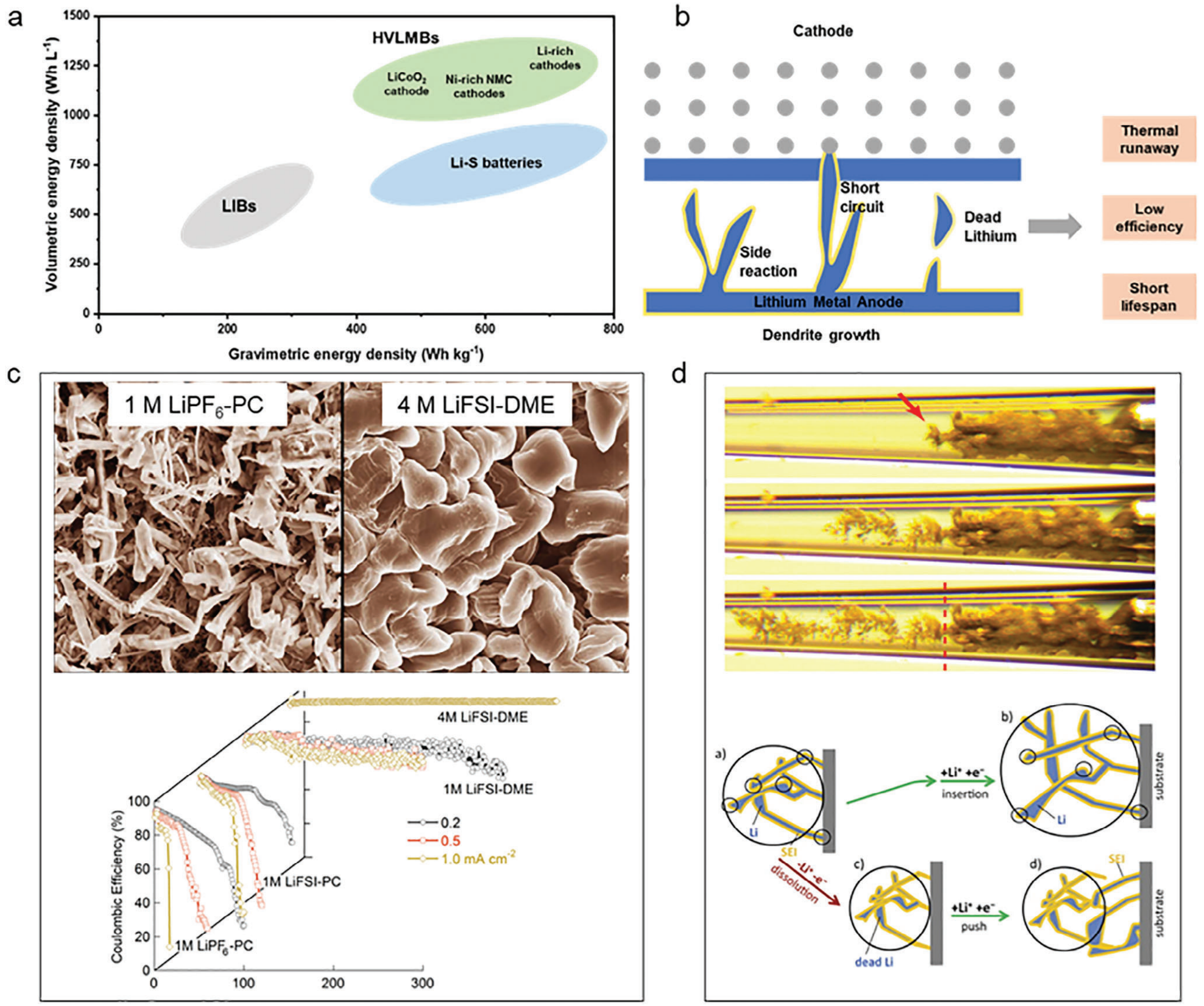

Figure 1. LMBs, electrolytes, and lithium dendrites. a) Gravimetric and volumetric energy densities of LMBs. b) The lithium dendrites and their detrimental effects. c) Comparison of the morphology and Coulombic efficiencies of Li-metal anode with the 1 M $LiPF_6$-PC and 4 M LiFSI-DME electrolytes. Reproduced with permission.[40] Copyright 2015, Nature Publishing Group. d) Schematic of suggested growth of Li^0 mossy structures. Reproduced with permission.[41] Copyright 2016, RSC Publishing. Reproduced with permission.[42] Copyright 2014, Elsevier.

electrolyte, especially under the practical conditions[13–16] including high cathode areal loading (e.g., >4 mAh cm^{-2}), lean electrolyte (electrolyte to capacity ratio, E/C ratio, e.g. <3 g Ah^{-1}) and low negative to positive capacity ratio (N/P ratio, e.g. <2), which are required for a high cell-level E_g. In other words, there is a trade-off between the E_g and cycle life for the practical LMBs. It is quite impressive to note that a record high E_g of 711.3 Wh kg^{-1} has recently been achieved by Li's group,[12] demonstrated by a 10 Ah Li||$Li_{1.2}Ni_{0.13}Co_{0.13}Mn_{0.54}O_2$ pouch cell with a cathode loading ~ 10 mAh cm^{-2}, an E/C ratio ~ 1.3 g Ah^{-1}, and an ultrathin 20 µm LMA.

To solve these issues, it is critical to manipulate the Li^0 deposition morphology and minimize the side reactions between Li^0 and electrolyte to achieve high-energy and long-lived LMBs. Mainly three effective strategies have been proposed: i) building artificial SEI[17–24] to regulate the Li^0 nucleation, deposition behavior, and SEI composition; ii) designing structured Li host to decrease the areal current density and to accommodate the volume change[25–32]; iii) electrolyte engineering to decrease its reactivity with Li^0 and to (in-situ) construct desired SEI on Li^0 surface.[33–36] Since the LMA is in direct contact with the surrounding electrolyte, the Li^0 deposition morphology and the side reactions are closely related to the electrolytes, which is analogous to metal electroplating. Till now, great research efforts have been devoted to developing new electrolytes for high-energy and long-lived LMBs.

In the present review, beginning with a brief overview of the fundamentals of the electrolyte–LMA relationship, we will pay particular emphasis on the recent key progress on new molecular designs for electrolyte components including new solvents, salts, and additives, which was seldomly discussed in previous reviews. To further concentrate our devotion, we mainly focus on the electrolytes for high-voltage LMBs (HVLMBs) using the intercalated-type cathodes including $\mathrm{LiNi}_x\mathrm{Mn}_y\mathrm{Co}_{1-x-y}\mathrm{O}_2$ (NMC) and LiCoO_2 (LCO). For other LMBs like Li–S batteries[15,37] using the conversion-type sulfur cathode, the electrolyte design strategy is different from the HVLMBs with particularly addressing the cross-talk of the lithium polysulfides (LiPS),[38] most of which is out of our scope. Just like the importance of the discovery of ethylene carbonate (EC) for the graphite anode,[39] we ought to believe that new electrolyte components are the key to the practical applications of the "fascinating but problematic" LMA. Furthermore, we will also discuss the electrolyte design rules, challenges, and underlying scientific problems for practical LMBs operating in practical environments from an industrial perspective, inspiring future electrolyte developments for LMBs.

2. Li^0 Electrodeposition and Its Relationship with Electrolyte

Li^0 electrodeposition process is influenced by numerous factors. Among them, Li^0 morphology and SEI compositions are greatly dictated by the interactions between Li^0 surface and electrolytes.[43] In the double layer near Li^0 surface, anions are often expelled by the electric field. According to Sand's classic theory,[44] a characteristic time t_{Sand} ("Sand's time") is used to describe the critical condition for Li^0 dendritic growth (Equation 1). When Li^+ cations are consumed by reduction reaction, a local zero-salt-concentration area will form, which depends on the competition between the applied current density and Li^+ diffusion.[41] Li^0 dendrites usually form due to the depletion of Li^+ cations near the electrode surface when the currents exceed diffusion limitation. Based on Eq. (1), the formation of the Li dendrites can be regulated by dynamic factors, including the current density, the ion diffusion/mobility, and so on.

$$t_{\mathrm{Sand}} = \pi D \left(\frac{CeF}{2Jt} \right)^2 \tag{1}$$

where D is the diffusion coefficient, C the bulk salt concentration, e the charge number of the cation (1 for Li^+), J the current density, F the Faraday constant (96485 C mol^{-1}), and t the transference number of the anion. Besides these basic diffusion characteristics of the electrolytes, the SEI derived from electrolyte reduction also obviously impacts Li^0 electrodeposition. The research on Li^0 nucleation[45] and growth behaviors in different electrolytes by multiple in-situ/ex-situ microscopy technologies[46,47] shows that electrolyte components including solvents, salts, and additives strongly affect the Li^0 morphology and the Li^0 plating-stripping CE. For example, the Li^0 electroplated from a propylene carbonate (PC)-based electrolyte tended to be needle-like and dendritic (Figure 1c). In contrast, the one electroplated from a 1,2-dimethoxyethane (DME)-based electrolyte tended to be a nodule-like structure with round-shaped edges (Figure 1c).[40] It could be attributed to the lower reactivity of the glyme solvents than the carbonate solvents. When dendritic Li^0 deposits dominate, dead Li^0 is easy to generate since the Li segment near the root is stripped preferentially and the rest Li lacks electrical contact with the electron source. The tip of the Li^0 whisker is detached and thus electrically isolated. This is the main reason for Li inventory loss and low CE (Figure 1d).

Goodenough et al. demonstrated that the SEIs form when the electrodes' redox potential is not within the electrolyte's electrochemical stability window (**Figure 2a**).[48] When the lowest unoccupied molecular orbital (LUMO) of the electrolyte is higher than the Fermi energy of anode, the electrolyte is stable; otherwise, the electrolyte can be reduced. Likewise, the electrolyte is expected to be stable if the highest occupied molecular orbital (HOMO) of the electrolyte is lower than the cathode's Fermi energy level. The composition of the SEIs in LMBs is mainly composed of Li-alkyl carbonate and inorganic composition (Figure 2b).[49] A range of SEI/cathode–electrolyte interface (CEI) structure models (e.g., mosaic structure (Figure 2c),[50] multilayer structure (Figure 2d),[51,52] and double-layer structure (**Figure 2e**)[53]) have been proposed. Li et al. demonstrated that the SEIs formed in the FEC-based electrolyte has a multilayer structure revealed by cryo-electron microscopy.[51] It is generally believed that by forming compact and electron-insulating SEIs/CEIs, the electrodes can be effectively protected and their side reactions with electrolyte can be minimized. In contrast to organic components, inorganic ones generally have low ionic diffusion rate, wide band gap, high surface energy, and high mechanical properties, making robust SEIs for accommodating the large volume change during Li–metal plating and stripping, effectively minimizing the side reactions between the LMA and the electrolyte. Therefore, it is essential to understand the electrolyte design principles for developing high-energy LMBs.

3. The Application of Classic Electrolytes in LMBs

Since the successful commercialization of LIBs in the 1990s, the electrolytes based on carbonate solvents and LiPF_6 salt have dominated the LIBs market due to their good compatibility with the graphite anode and high oxidation resistance to match the high-voltage cathodes. The output of carbonate-based electrolytes was beyond 1 000 000 tons in 2023, most of which were used in EVs, EESs, and digital products. However, due to the poor reduction resistance of the carbonyl group (−C=O−) in carbonates,[54] it is difficult to form stable SEIs between most traditional carbonates (e.g., EC, PC, methyl ethyl carbonate (EMC), diethyl carbonate (DEC), dimethyl carbonate (DMC)) and the LMA, leading to very low CE in LMBs.[55]

LiF is an excellent SEI passivation component to stop electron tunneling due to its large bandgap (13.6 eV) and to deform plastically by dislocation glide to maintain the structure and mechanical property of SEI.[56] LiF-rich SEI[33] can thus well stabilize the reactive Li^0 surface and constructing LiF-rich SEI becomes the key strategy to improve the compatibility of electrolytes with the LMA (**Figure 3a**). Therefore, fluorinated carbonates such as fluoroethylene carbonate (FEC),[57] Trans-difluoroethylene carbonate (DFEC),[58] methyl (2,2,2-trifluoroethyl) carbonate (FEMC),[59–61] and so on, that can induce abundant LiF components into SEI, are emerging for LMBs than the traditional fluorine (F)-free carbonates (will be discussed in Section 3.1.1).

Another classic electrolyte is the ether-based electrolyte. Although ethers (e.g., DME, 1,3-dioxolane (DOL)) are much less

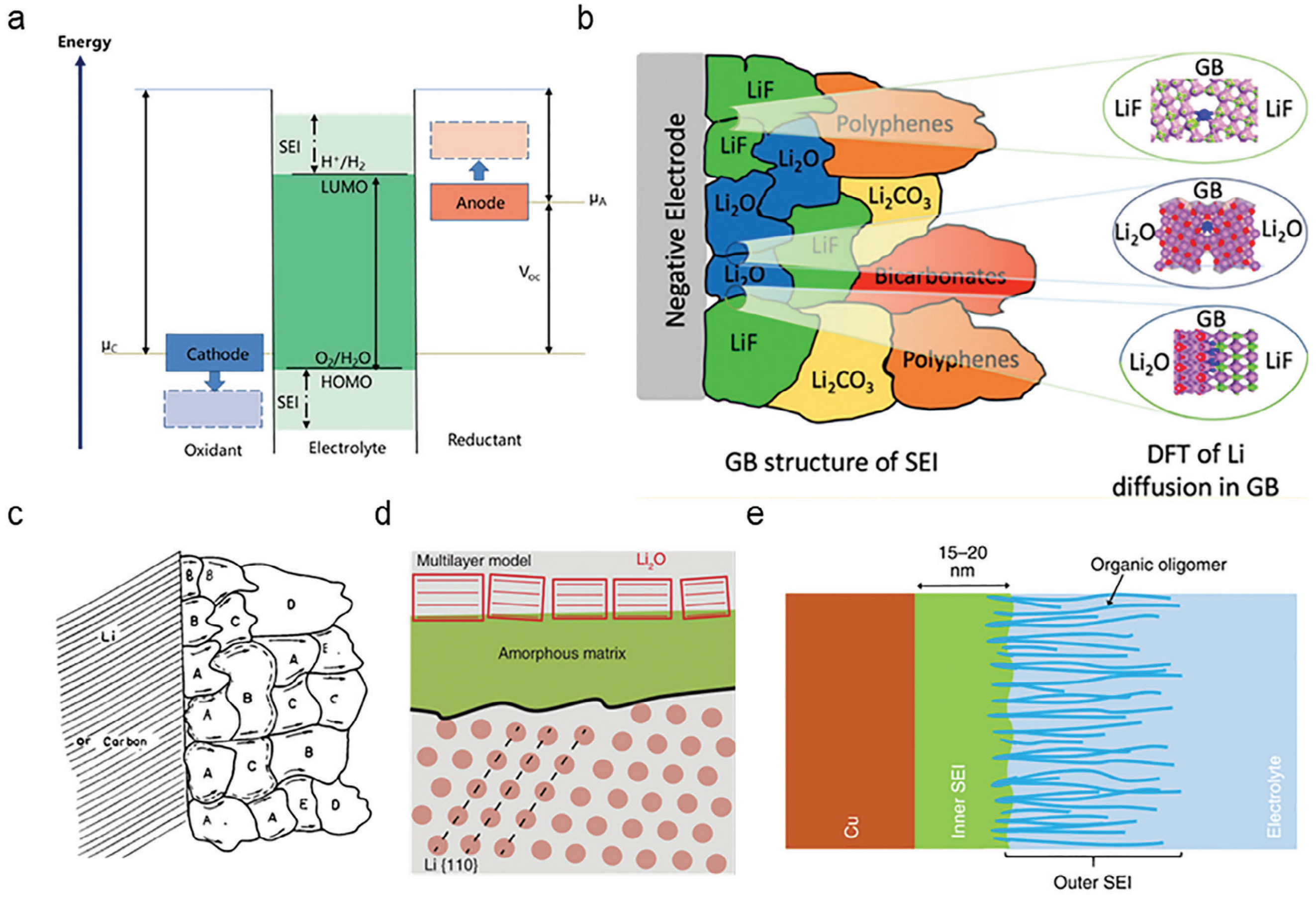

Figure 2. The composition and structural models of the SEI/CEI. a) Schematic energy diagram of an aqueous electrolyte. Reproduced with permission.[48] Copyright 2009, ACS Publishing. b) The composition structures of fluorinated SEI. Reproduced with permission.[49] Copyright 2019, ACS Publishing. c) Mosaic structure model. Reproduced with permission.[50] Copyright 1997, IOP Publishing. d) Multilayer structure model Reproduced with permission.[51] Copyright 2017, Science. e) Double-layer structure model. Reproduced with permission.[53] Copyright 2020, Nature Publishing Group.

prevailing in LIBs than carbonates due to their poor oxidation resistance <4 V versus (vs.) Li/Li$^+$, they exhibit great potential in LMBs mainly owing to their excellent reduction resistance against the reactive LMA.[62,63]

High salt concentration electrolytes (HCEs) and localized high salt concentration electrolytes (LHCEs) are effective ways to widen the electrochemical stability window of the ether-based electrolytes.[64–69] A generally accepted claim made on the mechanism is, in HCEs and LHCEs, the number of free solvent molecules and solvent-separated ion pair (SSIP) is decreased, with the contact ion pair (CIP) and aggregate (AGG) increased compared to the ~1 M salt concentration electrolytes (Figure 3b).[70] Consequently, more anions participate in the CEI/SEI formation with favorable inorganic (e.g., LiF) components, leading to higher Li–metal CE and better high-voltage stability(Figure 3c,d). Benefiting from these advantages, therefore, a lot of HCEs and LHCEs composed of classic F-free carbonates and ethers can work well in HVLMBs.[40,71–75] As both classic electrolytes are well discussed in previous works,[76–80] in our present review, we will particularly focus on the electrolytes composed of newly-designed molecules.

4. Molecular Engineering of New Electrolytes for HVLMBs

To solve the issues in LMBs, molecular engineering for new electrolyte components has attracted lots of attention recently. It means the design and synthesis of novel molecules with desirable physical properties or functionalities. The molecular structures of electrolyte components have a great influence not only on their own physicochemical properties but on the Li$^+$ solvation structure, their decomposition pathways, SEI/CEI compositions/properties, LMA compatibility, and thus the electrochemical performance as well. In this section, we will focus on the molecular engineering for key electrolyte components including designing new solvents, salt, and additive molecules.

4.1. Solvent Molecular Engineering

4.1.1. Fluorinated Carbonates

Fluorinated carbonates (**Figure** 4a) have been widely reported as favorable electrolyte solvents for LMBs. Due to the strong

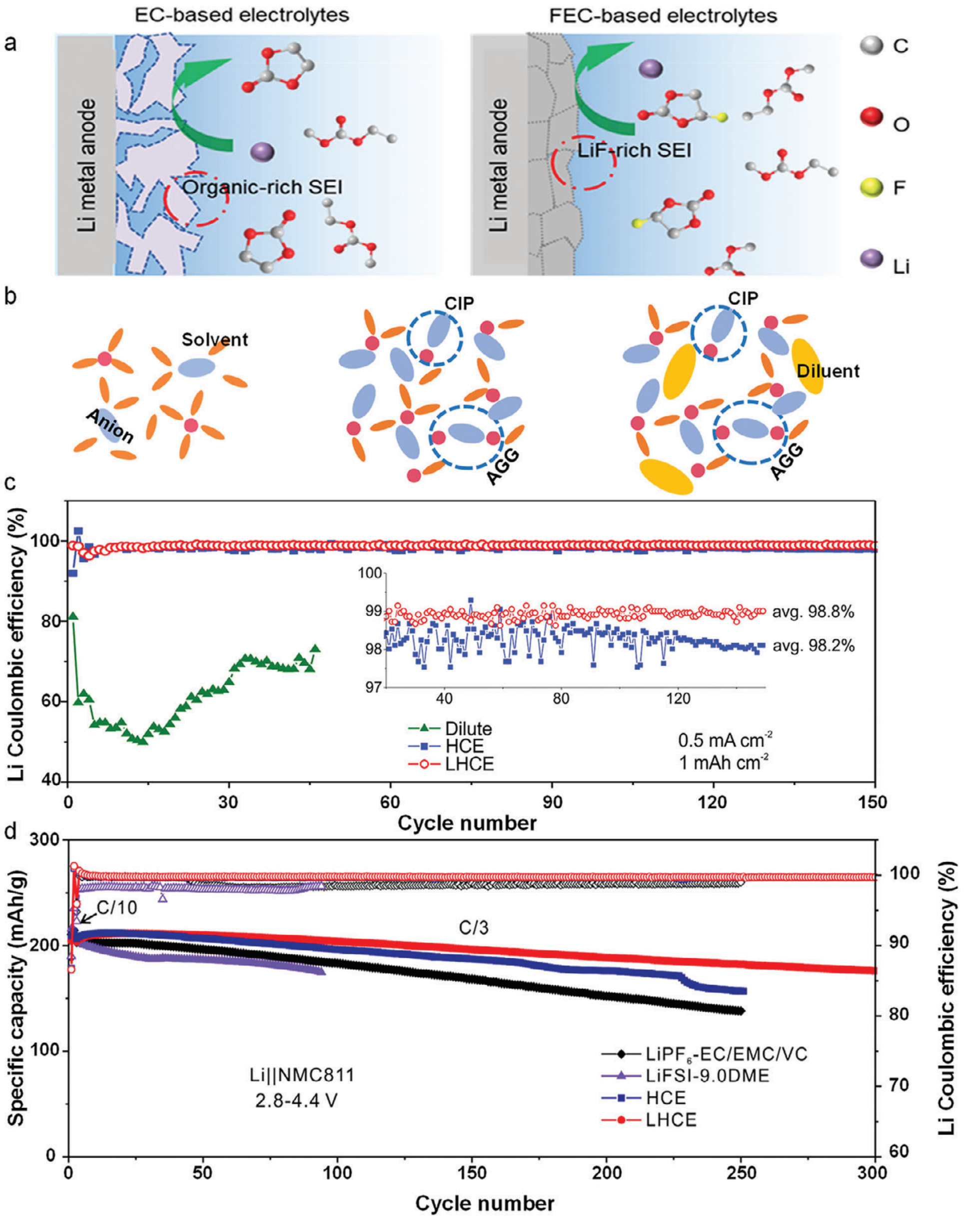

Figure 3. The application of classic electrolytes in LMBs. a) Schematic illustration of the SEI formation in EC-based electrolytes and FEC-based electrolytes. b) Solvation structure of the conventional electrolytes, the HCEs, and the LHCEs. c) Li–metal CEs in a tetramethylene sulfone (TMS)-based dilute/HCEs/LHCEs electrolytes. Reproduced with permission.[66] Copyright 2018, Elsevier. d) Cycling performance of Li||NMC811 batteries in a carbonate-based conventional electrolyte, LiFSI-DME-based HCEs, and LiFSI-DME-TTE-based LHCEs at an upper cut-off voltage of 4.4 V. Reproduced with permission.[81] Copyright 2019, Elsevier.

electronegativity of the F atom, F-contained groups (FCGs), for example, –F, –CF_3, or –CHF_2, have strong electron-withdrawing effects. The introduction of FCGs into molecules would generally shift down the LUMO andHOMO energy levels, corresponding to higher oxidation resistance and lower reduction resistance, respectively (Figure 4b). Despite the weakened reduction resistance after fluorination, LiF-rich SEI can be generated upon the reduction of fluorinated carbonates, thus improving the compatibility with the LMA. Meanwhile, the stereochemical structure of fluorinated carbonates, such as the number and substitution positions of fluorine atoms, can influence the physicochemical properties of electrolytes and the generated SEI, which eventually dictates the cycling performance of LMBs.

So far, fluorinated carbonates in LMBs can be mainly classified into two categories (**Figure** 4a):

1) *Cyclic fluorinated carbonates.* As a typical cyclic carbonate, FEC[56] is a common additive in LIBs to generate fast-Li^+-conductive SEI on the graphite anode[82] and to form robust SEI on silicon-based anodes to accommodate their huge volume change during lithiation–delithiation.[83] It is also a very useful additive/co-solvent for improving the electrolyte

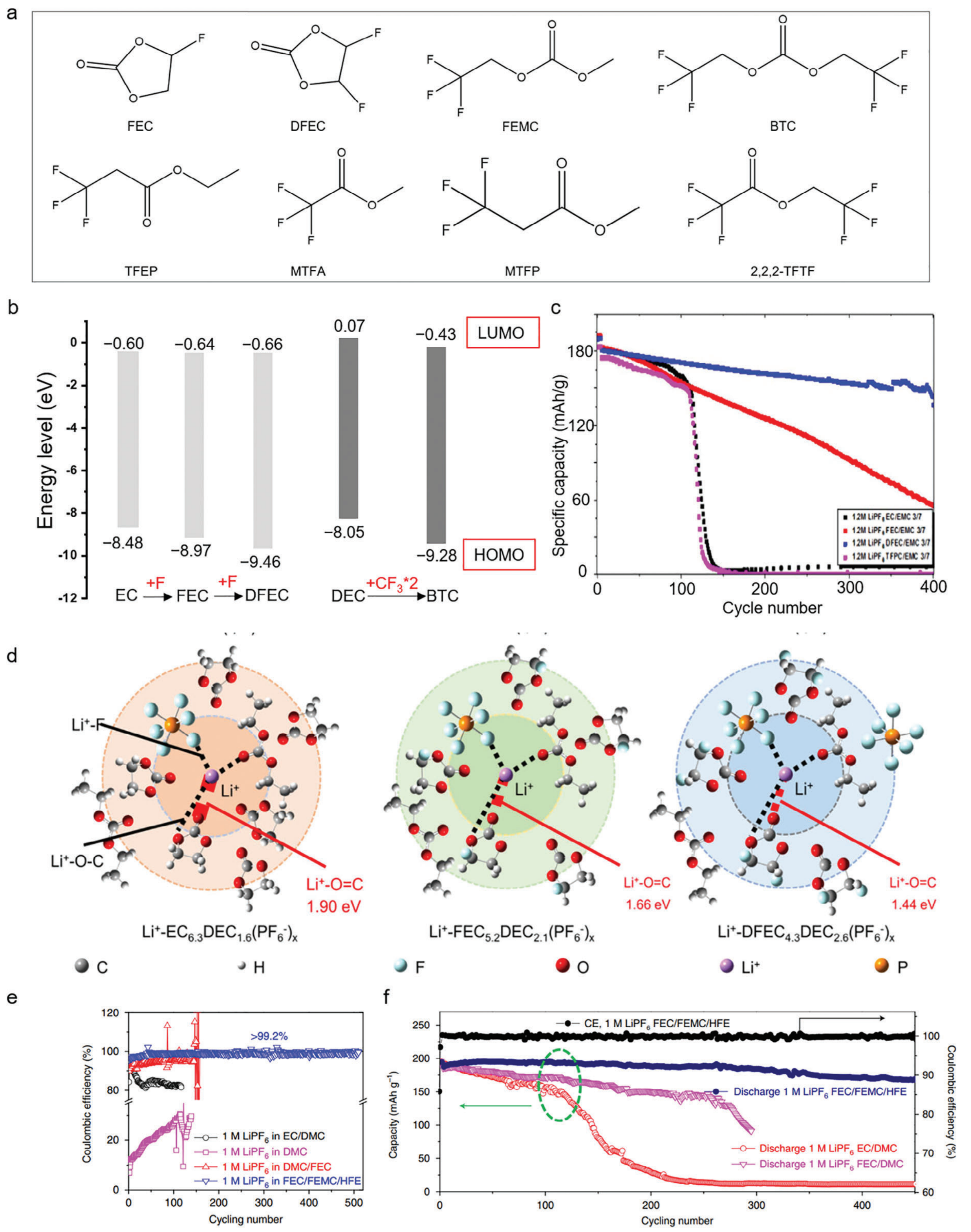

Figure 4. Effect of introducing F into carbonate molecules on the molecular orbital energy levels and the interaction with Li$^+$. a) Molecular structures of the fluorinated carbonates. b) Molecular orbital energies of different solvents. c) Cycling performance of Li||NMC622 cells using 1.2 M $LiPF_6$ in EC/EMC, FEC/EMC, DFEC/EMC, and TFPC/EMC electrolytes (3/7 v) at room temperature. Reproduced with permission.[85] Copyright 2019, Elsevier. d) Schematics of the Li$^+$ solvation structure in the 1 M $LiPF_6$-EC/DEC, 1 M $LiPF_6$-FEC/DEC, and 1 M $LiPF_6$-DFEC/DEC electrolytes. Reproduced with permission.[87] Copyright 2021, Wiley-VCH. e) Li plating/stripping CE of Li||Cu cell with the 1 M $LiPF_6$ in FEC:FEMC:HFE (2:6:2 w) electrolyte at 0.2 mA cm^{-2}. Reproduced with permission.[89] Copyright 2018, Nature Publishing Group. f) Cycling stability of Li||NMC811 cells with the 1 M $LiPF_6$ in FEC:FEMC:HFE (2:6:2 w) electrolyte at a cut-off voltage of 4.4 V. Reproduced with permission.[89] Copyright 2018, Nature Publishing Group.

compatibility with the LMA.[84] Besides FEC, Amine et al. found that the electrolyte with DFEC as solvent, featuring more F-atoms compared to FEC, enabled much higher capacity retention (82%) than an FEC-based electrolyte (31%) evaluated by Li||NMC622 cells (Figure 4c).[85] Furthermore, the Li^+–solvent bonding could be weakened by introducing DFEC (Figure 4d), promoting Li^+ desolvationand thuselectrochemical kinetics. This is very important for low-temperature operation of LMBs.[86] A DFEC-based electrolyte proposed by an ion–dipole strategy was reported.[87] It enabled a six-time faster Li^+ desolvation rate than that of an EC-based electrolyte at −20 °C and ≈51% room-temperature capacity can be retained even at −30 °C.

Linear fluorinated carbonates. Recently, Suo et al. proposed a fluorinated linear carboxylic ester (ethyl-3,3,3-trifluoropropionate, tFEP) together with FEC and $LiBF_4$/LiDFOB to induce more anions into the inner Helmholtz plane near the LMA surface, thus prompting the formation of anion-derived SEI and high Li-metal stripping-plating CE of ~98.7%.[88] Impressively, benefiting from this electrolyte, an industrial-level anode-free 4.6-V-class Cu||NCM811 pouch cell can deliver an energy density of 442.5 Wh kg^{-1} with 80% capacity retention after 100 cycles. Other fluorinated solvents were also proposed to work synergistically to support both the aggressive LMA and high-voltage cathodes. In 2018, Fan et al. reported a 1 M $LiPF_6$ /FEC: FEMC: HFE (1,1,2,2-tetrafluoroethyl-2′,2′,2′-trifluoro-ethyl ether) in a weight ratio of 2:6:2.[89] This electrolyte successfully enabled high CE ≈99.2% for Li–metal plating/stripping, ≈99.81% for 5 V $LiCoPO_4$, and ≈99.93% for NMC811, respectively (Figure 4e,f). This was a pioneering electrolyte-designing strategy for HVLMBs with $LiPF_6$ as salt that can overcome the corrosion issue of sulfonamide-type LiTFSI/LiFSI salts frequently used for LMBs. By adopting two $-CF_3$ groups into both ends of the carbon chain in DEC, a new solvent bis(2,2,2-trifluoroethyl) carbonate (BTC) was reported by Cheng's group.[90] The BTC-based electrolyte exhibited substantially enhanced high-voltage stability, which can enable NCM811 at ultrahigh cut-off voltages up to 4.8 V vs. Li/Li^+. A high Li–metal plating-stripping CE in this electrolyte guarantees the Li||NCM811 cell with a high capacity retention of ≈81.3% after 120 cycles with an E/C ratio of ≈7 g Ah^{-1}. Other fluorinated linear carbonates,[91] e.g., methyl trifluoroacetate MTFA,[92] methyl 3,3,3-trifluoropionate MTFP,[93] and 2,2,2-trifluoroethyl trifluoroacetate (2,2,2-TFTF),[94] were also reported (Figure 4a).

4.1.2. New Ether Molecules

As discussed in Section 2, although the high reduction resistance of the classic ethers can be leveraged in LMBs, their poor oxidation stability is problematic when matching 4-V/5-V-class cathodes. So far, several effective strategies based on molecular engineering have been reported (**Figure 5a**) to enhance their high-voltage stability and their performance in LMBs.

Regulating the Alky Chains: Alky chains in ether molecules have an impact on their high-voltage stability, Li^+ dissociation, and desolvation ability.[95–98] By shortening the alky chain between two oxygen atoms of the DME molecule, dimethoxymethane (DMM) was proposed to possess weaker solvating ability and lower energy barrier for desolvation than DME, which allows uniform Li deposits and higher Li–metal CE of 97.87% at −40 °C, compared to only 44.68% for DME.[99] By extending the alky chain of the DME molecule, the as-yielded 1,2-diethoxyethane (DEE) could weaken the bonding of Li^+–$(\text{solvent})_n$ complexes.[100,101] Liu et al. discovered that the Li||Cu cell with 1 M LiFSI-DEE electrolyte maintained an average CE of ≈98.4% at −60 °C, compared to ≈27.5% at the same temperature with 1 M LiFSI/DME–DOL electrolyte[102] (Figure 5b). Lee et al. attributed the better Li–metal CE with the LiFSI–DEE electrolyte (than with the LiFSI–DME electrolyte) to the Li^+ solvation structure similar to HCEs.[101] Moreover, it is effective in replacing the vulnerable α-H atom in DEE with a methyl group for enhancing its high-voltage stability, yielding a new ether molecule 1,2-diethoxypropane (DEP).[103] Impressively, the 4.3-V-class anode-free Cu||$LiNi_{0.8}Co_{0.15}Al_{0.05}O_2$ (NCA) pouch cell with the 2 M LiFSI–DEP electrolyte exhibited a record cycle life of 250, which can be attributed to the unique compatibility of the electrolyte with both the LMA and the high-voltage NCA cathodes. Furthermore, by inserting a $-CH_2-$ into the DME molecule, Ren et al.[104] designed a new ether molecule, 1,3-dimethoxypropane (DMP), which enables high Li^+ conductivity and excellent oxidation resistance. Benefiting from the unique six-membered chelating complex with Li^+, the DMP-based electrolyte can be operated in 4.7 V Li||NMC811 cell (Figure 5c) with high-rate performance up to 4 C and high cycling stability (85% retention after 100 cycles) under practical battery conditions (cathode loading ~ 4.0 mAh cm^{-2}, N/P ratio ~ 2.4) (Figure 5d,e).

Long-Chain Ethers: By increasing the number of ethylene glycol monomers, the oxidation stability can be improved.[105] Diethylene glycol dimethyl ether (DEGDME, G2), Triethylene glycol dimethyl ether (G3), and tetraethylene glycol dimethyl ether (TEGDME, G4) are typical examples of long-chain ethers, which are popular in $Li-O_2$ batteries due to their good resistance against attack by oxygen radicals.[106–108] Chen et al. studied the G2, G3, and G4-based LHCEs and found that the G3-based LHCE (LiFSI: G3: 1,1,2,2-tetrafluoroethyl 2,2,3,3-tetrafluoropropyl eher (TTE) = 1:1:3 mol) with the highest Li^+ solvation energy showed the best cycling stability (93% capacity retention after 100 cycles) with 4.7 V single-crystalline NMC811 cathode among all the LHCEs they investigated . In addition, an average Li–metal CE of 99.3% was achieved because of the preferred reduction of FSI^- anions and the stability of G3 with the LMA.[109]

Partially Fluorinated Ethers: It is an effective strategy to introduce electron-withdrawing groups (e.g., –F or $-CF_3$, –C≡N) into ether molecules for enhancing their oxidation resistance without compromising the LMA compatibility. Unlike the highly fluorinated ethers used as noncoordinated diluents (NCD) in LHCEs (e.g., bis(2,2,2,-trifluoroethyl) ether (BTFE), TTE),[68,65] partially fluorinated ethers can coordinate with Li^+ and participate in the Li^+ solvation sheath, so-called the weak-coordinated diluent (WCD, **Figure 6a**), which significantly promoted the formation of inorganic-rich SEI.[110,111]

In 2020, Yu et al.[112] pioneered the incorporation of $-CF_2-$ units into the 1,4-dimethoxylbutane (DMB) molecule creating a new fluorinated 1,4-dimethoxylbutane (FDMB) molecule even without a CAS number at that moment (Figure 6b). The resultant single-solvent single-salt electrolyte 1 M LiFSI/FDMB formed Li–F binding between the Li^+ and the FDMB molecule with a high anion/solvent ratio in the solvation sheath (increased from

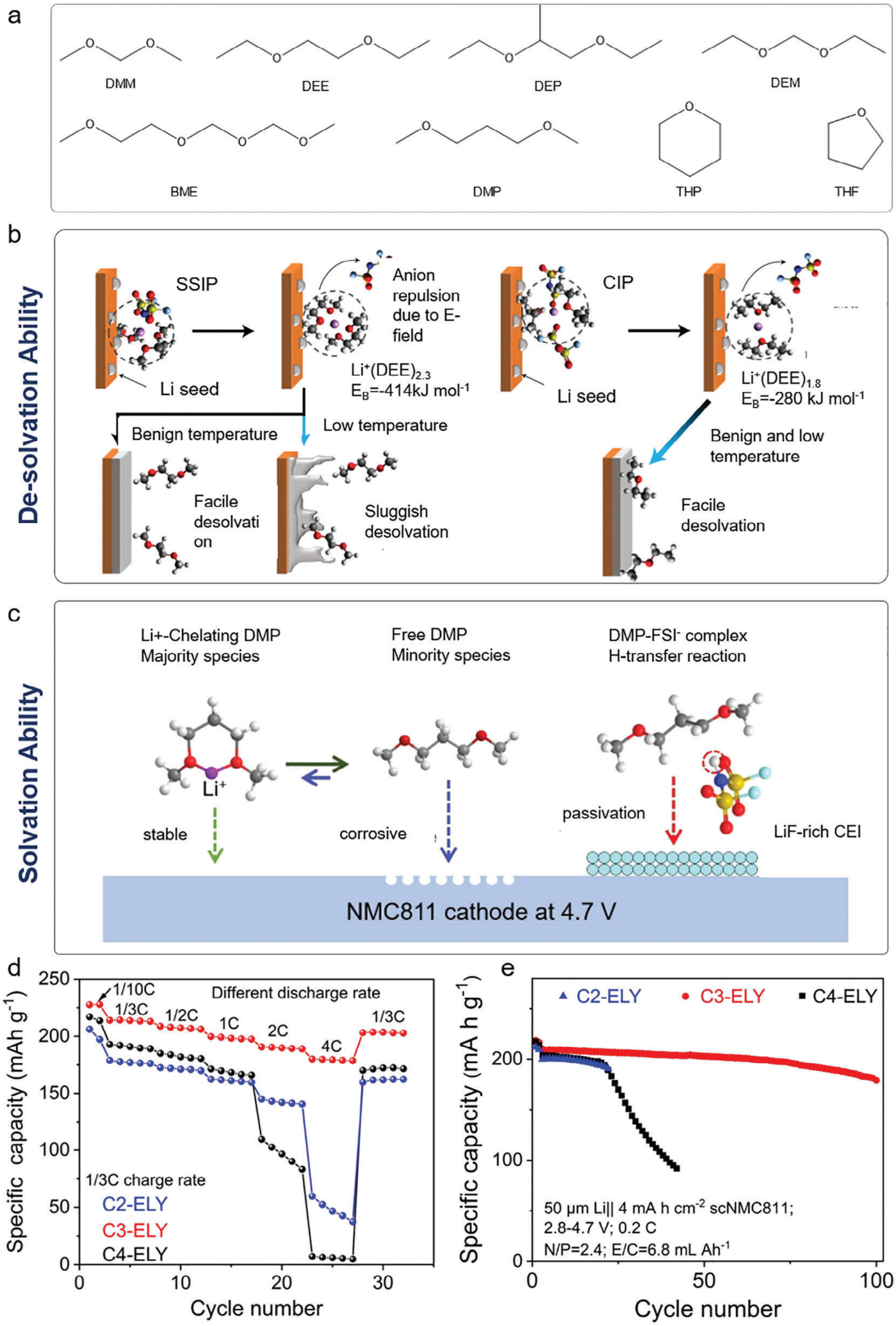

Figure 5. Molecular engineering for regulating the alky chains in ether molecules. a) Molecular structures of the modified ethers. b) Proposed desolvation mechanisms in the DEE-based electrolyte. Reproduced with permission.[102] Copyright 2021, Nature Publishing Group. c) Proposed higher solvation ability in the DMP-based electrolyte. d) Rate capabilities of Li||NMC811 (2 mAh cm^{-2}) batteries in the DMP-based electrolyte under varied discharge rates with constant charge rate at C/3. e) Cycling performances of Li||NCM811 (4.0 mAh cm^{-2}, N/P = 2.4) using DMP-based electrolyte. Reproduced with permission.[104] Copyright 2023, Wiley-VCH.

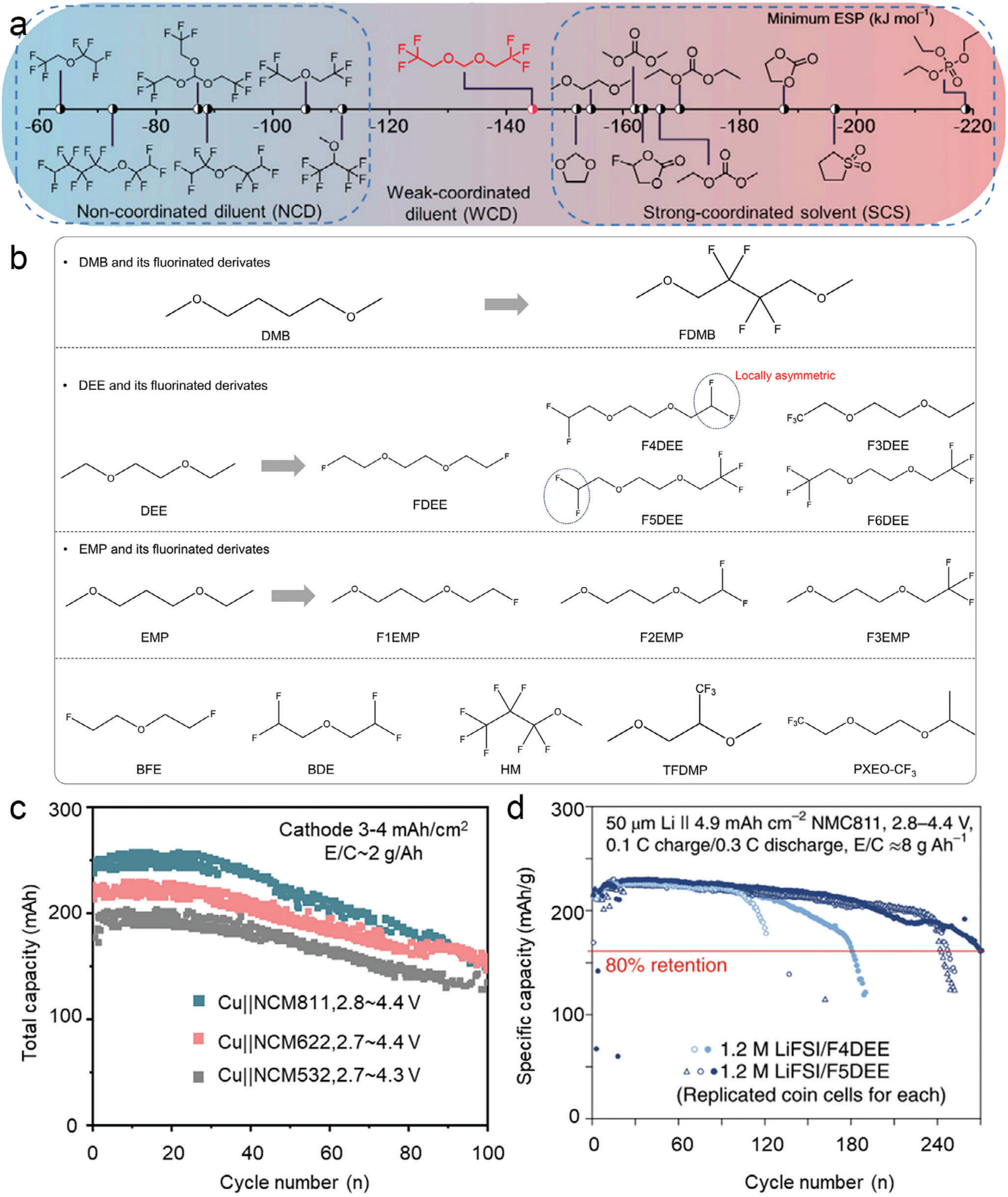

Figure 6. Molecular engineering for introducing electron-withdrawing groups into ether molecules. a) Calculated minimum electrostatic potentials (ESPs) corresponding to NCD, WCD, and strong-coordinated solvent (SCS). Reproduced with permission.[110] Copyright 2023, Elsevier. b) Molecular structures of the partially fluorinated linear ethers. c) Cycling performance of anode-free pouch cells (4.0 mAh cm^{-2}, N/P = 0) cells cycled with the FDMB-based electrolytes. Reproduced with permission.[112] Copyright 2020, Nature Publishing Group. d) Cycling performance of Li||NCM811 cells using the F5DEE-based electrolyte at a cut-off voltage of 4.4 V. Reproduced with permission.[113] Copyright 2022, Nature Publishing Group.

2.31 to 3.29), achieving a high average Li-metal plating/stripping CE ~99.52%. Impressively, it exhibited outstanding oxidation resistance to match NMC cathodes at high cut-off voltages up to 4.6 V vs. Li/Li$^+$. Highly stable anode-free Cu||NMC pouch cells were thus attained with 80% capacity retention for 100 cycles under practical conditions (cathode loading ~ 4 mAh cm^{-2} and E/C ratio ~ 2 g Ah^{-1}, Figure 6c). Afterward they developed a family of fluorinated DEE by tuning the fluorination degree (F (3–6) DEE molecules). Electrolyte performance including the ionic conductivity, the overpotential of Li^0 deposition, and the resultant performance of anode-free pouch cells are found to be closely related to the position and the amount of F atoms in the solvent molecules.[113,114] The electrolyte based on the F5DEE molecule bearing two –CHF$_2$ groups reached extremely high Li–metal CE (≈99.90% in 1.2 M LiFSI/F5DEE) together with high ionic conductivity (5.01 mS cm^{-1}) and high-voltage stability (4.4 V vs. Li/Li$^+$) (Figure 6d). Wu et al. subsequently proved that the local polar –CHF$_2$ group is effective as a desired functional group in the 1-methoxy-3-ethoxypropane (EMP) system.[114] Further testing with full cells using a high-voltage (4.4 V) and high-loading (≈3.9 mAh cm^{-2}) NCM811 cathode indicated that the F2EMP-based (Figure 6b) electrolyte results in 80% capacity retention after 168 cycles with limited Li (50 µm). So far, numerous new fluorinated ethers have been developed, which achieved excellent compatibility with both the LMAs and the high-voltage cathodes including 1,2-bis(2-fluoroethoxy) ethane (FDEE),[115] bis (2,2-difluoroethyl) ether (BFE),[116] bis (2,2-difluoroethyl) ether (BDE),[116] heptafluoro-1-methoxypropane (HM),[117] 1,1,1-trifluoro-2,3-dimethoxypropane (TFDMP)[118] and ethylene glycol (2,2,2-trifluoroethyl-i-propyl) ether (PXEO-CF$_3$) (Figure 6b).[119]

In addition to the above-mentioned linear ethers, classic cyclic ethers like DOL are commonly used in LMBs featuring its in-situ ring-opening polymerization to protect the LMA.[115,120] To enhance their oxidation stability,[121] Coskun's group designed a series of cyclic ether molecules with –CF$_3$ groups, such as 2,2-dimethoxy-4-(trifluoromethyl)-1,3-dioxolane (DTDL), 2-ethoxy-4-(trifluoromethyl)-1,3-dioxolane (cFTOF), 4-(trifluoromethyl)-1,3-dioxolane (TFDOL) and 2-(2,2,2-trifluoroethoxy)-4(trifluoromethyl)-1,3-dioxolane (TTD)(**Figure 7**a).[122–126] Incorporating electron-withdrawing functional groups into the DOL molecule results in a decrease in its HOMO energy level (Figure 7b). Electrolytes based on these new molecules showed greatly enhanced oxidation resistance that can operate well in Li||NMC batteries with high cut-off voltages ranging from 4.3 to 4.7 V vs. Li/Li$^+$. They also exhibited excellent stability to suppress harmful side reactions with the LMA, which is reflected by the high Li–metal plating/stripping CEs >99% (Figure 7c). Very recently, Li et al. designed a highly fluorinated cyclic ether (3,3,4,4,5,5-hexafluorotetrahydropyran, HFTHP) as a diluent to develop a dual-salt LHCE, 1 M LiDFOB and 0.4 M LiBF$_4$ in DME/HFTHP.[127] In contrast to the classic diluents BTFE and TTE, HFTHP has a much weaker Li$^+$ coordination capability, promoting the formation of a bilayer SEI, a Li$_2$O-rich inner layer, and a LiF-rich outer layer. Such an electrolyte successfully enabled a high cell-level E_g of 410 Wh kg^{-1} and long cycle life of 470 cycles demonstrated by a 0.1 Ah Li||NMC811 pouch cell at a high cathode loading ~ 4 mAh cm^{-2}, E/C ratio ~ 2.4 g Ah^{-1}, and a cut-off voltage of 4.3 V (Figure 7d).

High-Degree Fluorinated Ethers Without Coordination with Li$^+$: In 2015, Moon et al. found that TTE hardly participated in the Li$^+$ solvation shell because of its low donor ability resulting from its highly symmetric and nonpolar molecular structure.[128] By introducing such kind of highly fluorinated ethers into HCEs as an "inert" diluent, Zhang and Xu's group proposed a class of LHCEs[129] to reduce the overall salt concentration and viscosity of HCEs without compromising the excellent compatibility with high-voltage cathodes and the LMA. Besides TTE,[130,131] so far, a series of diluents have been discovered, such as tris(2,2,2-trifluoroethyl) orthoformate (TFEO),[132,133] 2,2,2-trifluoroethyl 1,1,2,2-tetrafluoroethyl ether (TFTFE),[134] 1H,1H,5H-octafluoropentyl 1,1,2,2-tetrafluoroethyl ether (OFE)[135] and BTFE[65,129] (**Figure 8**a). Ren et al. reported an LHCE (LiFSI:DME:TTE = 1:1.2:3 in molar ratio) enabling anode-free Cu||NMC811 cells with 77% capacity retention for 70 cycles under practical conditions including a high cathode loading ~ 4.2 mAh cm^{-2} and an E/C ratio ≈3 g Ah^{-1} (Figure 8b).[81] Afterward, he and his colleagues[136] further improved the high-voltage stability of this LHCE by reducing the interfacial reactivity of free ether solvents, yielding a series of new LHCEs, MADE-1–MADE-3 (LiFSI:DME:TTE = 1:9:27 (≈0.19 M), 2:9:27(≈0.38 M), and 3:9:27 (≈0.56 M) in molar ratio). A molecular anchoring approach[136] was thus proposed and the MADE series electrolytes successfully enabled 4.7 V Li||NMC811 cells with excellent cycling performance. Specifically, the cell with MADE-electrolyte could maintain a capacity retention of >86% over 100 cycles, compared to a much lower specific capacity and retention of 42% over 100 cycles with the traditional LHCE electrolyte (Figure 8c).

4.1.3. Sulfonamides

The transition from the classic graphite anode to the LMA with more aggressive chemistry opens a new avenue for new electrolytes outside the prevailing carbonate and ether-based electrolytes. So far it has become a hot topic to design new electrolyte molecules for LMBs not only including the derivates from carbonate and ether molecules, but also for other kinds of new molecules. An explicit molecular design strategy, therefore, is quite required.

In 2020, Xue et al.[137] pioneered a "salt-structure-mimicking strategy" (SSM strategy) by imitating the fluorosulfonyl imide group from a well-known LMA-compatible salt, LiFSI. They thus successfully developed a new organic solvent molecule dimethylsulfamoyl fluoride (DMSF, **Figure 9**a), which belongs to the sulfonamide family outside the carbonates and ethers family. Density functional theory (DFT) calculations revealed that the F atom in the DMSF molecule is more favorable to form LiF on the LMA surface than the traditional FEC molecule. By coupling with 2.5 m (molality, mole salt in kilogram solvent, mol kg^{-1}) LiFSI, a medium salt concentration electrolyte, so-called a "full fluorosulfonyl" (FFS) electrolyte, was yielded, It successfully enables high average Li metal CE ~ 99.03% with favorable large, uniform and compact Li deposits (Figure 9b). Benefiting from the electron-withdrawing effect from both –F and O=S=O groups, the FFS electrolyte exhibited high anodic stability and enabled Li||NCM622 cell with limited Li inventory to

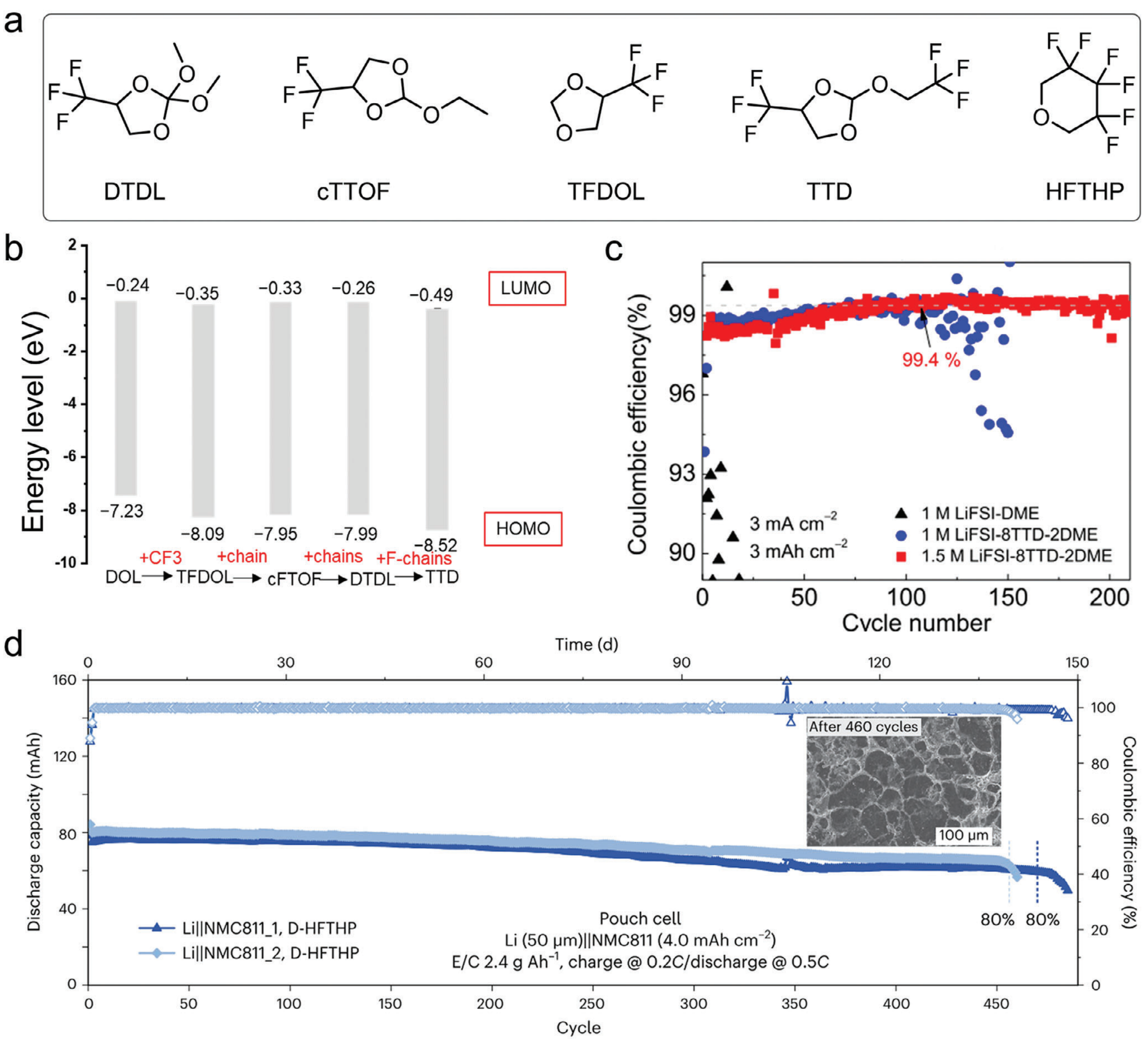

Figure 7. Molecular engineering for introducing electron-withdrawing groups in cyclic ether molecules. a) Molecule structures of several fluorinated cyclic ethers. b) Molecular orbital energies of different solvents. c) Li–metal CE of Li||Cu cells using the TTD-based electrolyte at 3 mA cm^{-2} & 3 mAh cm^{-2}. Reproduced with permission.[125] Copyright 2022, ACS Publishing. d) Cycling performance of Li ||NMC811 pouch cells between 2.8 and 4.3 V at room temperature and E/C raio of 2.4 g Ah^{-1} with the D-HFTHP-based electrolyte. Reproduced with permission.[127] Copyright 2024, Nature Publishing Group.

retain 89% of its original capacity after 200 cycles (Figure 9c). Guided by the SSM strategy, another sulfonamide molecule *N,N*-dimethyltrifluoromethanesulfonamide (DMTMSA) with similar molecular structure as LiTFSI was developed.[138,139] Impressively, the regular concentration 1 m LiFSI/DMTMSA electrolyte successfully enabled stable cycling of polycrystalline NCM811 at an ultrahigh cut-off voltage of 4.7 V (vs Li$^+$/Li). A high initial specific capacity of >230 mAh g^{-1} and superior capacity retention of 88.1% after 100 cycles were achieved, compared to only 76.1% capacity retention after 100 cycles using the carbonate-based electrolyte. The 1 m LiFSI/DMTMSA electrolyte greatly reduced the detrimental side reactions at high voltages in terms of gas releasing and transition metal dissolution. The intergranular cracking between the NCM811 primary particles, which is known to be a main degradation cause during high-voltage cycling, was also observed to be relieved. Stemming from the strong electron-withdrawing groups –CF$_3$ and O=S=O and the weakly solvating effect of the DMTMSA molecule, the amount of corrosion species near the cathode surface could be reduced to inhibit the stress-corrosion cracking (SCC) of the NCM811 cathode (Figure 9d). Furthermore, the 1 m LiFSI/DMTMSA electrolyte showed excellent LMA compatibility with desirable Li morphology, minimized Li metal pulverization, and high Li–metal CE >99% (Figure 9e). Under harsh practical conditions including

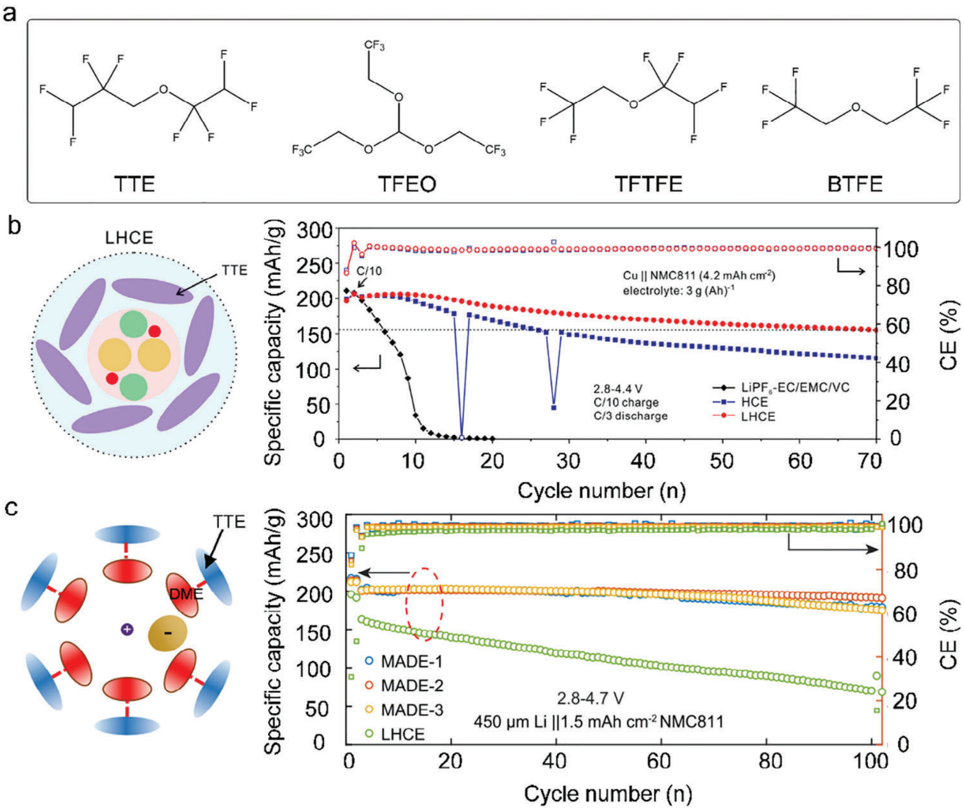

Figure 8. Molecular engineering for noncoordinated ethers. a) Molecular structures of several fluorinated ethers. b) Solvation structure of the TTE-based electrolyte and cycling performance of anode-free cells (4.2 mAh cm^{-2}, N/P = 0) cells. Reproduced with permission.[81] Copyright 2019, Elsevier. c) Solvation structure of the MADE electrolyte and cycling performance of Li||NCM811 (N/P = 2.1) cells. Reproduced with permission.[136] Copyright 2024, Nature Publishing Group.

≈5 mAh cm^{-2} cathode, 2.6 g Ah^{-1} electrolyte, and N/P ratio ~ 0.4, the practical 4.7 V Li||NMC811 cell can retain >88% capacity for 90 cycles (Figure 9f). Furthermore, the degradation mechanism of the cathode surface in the DMTMSA-based electrolyte was studied using single-crystalline LiCoO$_2$ as cathode.[139] High-voltage stability of the LCO cathode up to 4.6 V vs. Li/Li$^+$ can be achieved in this electrolyte, outperforming the traditional carbonate-based electrolyte. It can be explained by the protective CEI formed at 4.0 V, which maintains stable up to 4.8 V. The sulfonamide solvent family has become promising in boosting the performance of HVLMBs, and has attracted lots of attention recently.

Until now, two approaches have been reported to develop new sulfonamides derived from DMTMSA. One approach is to extend the fluorine chain, for example, CF$_3$(CF$_2$)$_2$– to replace the –CF$_3$ group yielding a new sulfonamide molecule, nonafluoro-*N*,*N*-dimethylbutane sulfonamide (NFS) featuring an Li$^+$ dissociative polar head and a perfluorinated nonpolar tail.[140] The long fluorine chain in NFS decreased the solvation capability and promoted the formation of capsule-like solvation sheaths with DME as a co-solvent, which dissociates the lithium salt. The NFS-based electrolyte enabled 420 mAh pouch cell with a cell-level energy density of 440 Wh kg^{-1} and ≈92% capacity retention after 150 cycles. The other approach is to modify the carbon chain by introducing ring structures to DMTMSA, yielding 1-(trifluoromethyl) sulfonyl) piperidine (TFSPP)[141] and *N*-pyrrolidine-trifluoromethanesulfonamide (TFSPY)[142] (**Figure 9a**). Fan et al. recently demonstrated the optimal reductive stability of TFSPY by evaluating the qualitative relationship between electronegativity and electrophilicity or coordination ability. The TFSPY-based electrolyte successfully enabled anode-free Cu||NCM523 pouch cells with 82% of capacity over 100 cycles.[142]

As a new solvent family, sulfonamides possess physiochemical properties suitable for electrolytes including high boiling point, low viscosity, good wettability, wide electrochemical stability window, and good compatibility with the LMA. By synergizing with other solvents, salts, and additives, we ought to believe that sulfonamide-based electrolytes would be promising for high-energy LMBs.

4.1.4. Silanes

A series of silanes have been reported as new electrolyte solvents for LMBs, featuring their lower density (≤1 g cm^{-3}) than most carbonates (≈1.2 g cm^{-3}) that benefits high cell-level E_g (**Figure 10a**). The presence of Li$_x$Si-contained SEI derived from the decomposition of silanes could favor the Li$^+$ conductivity, helping uniformize the Li^0 deposition. Suo's group reported a new (trifluoromethyl)trimethylsilane (TFMTMS) solvent molecule with a low density of 0.96 g cm^{-3}. The as-yielded

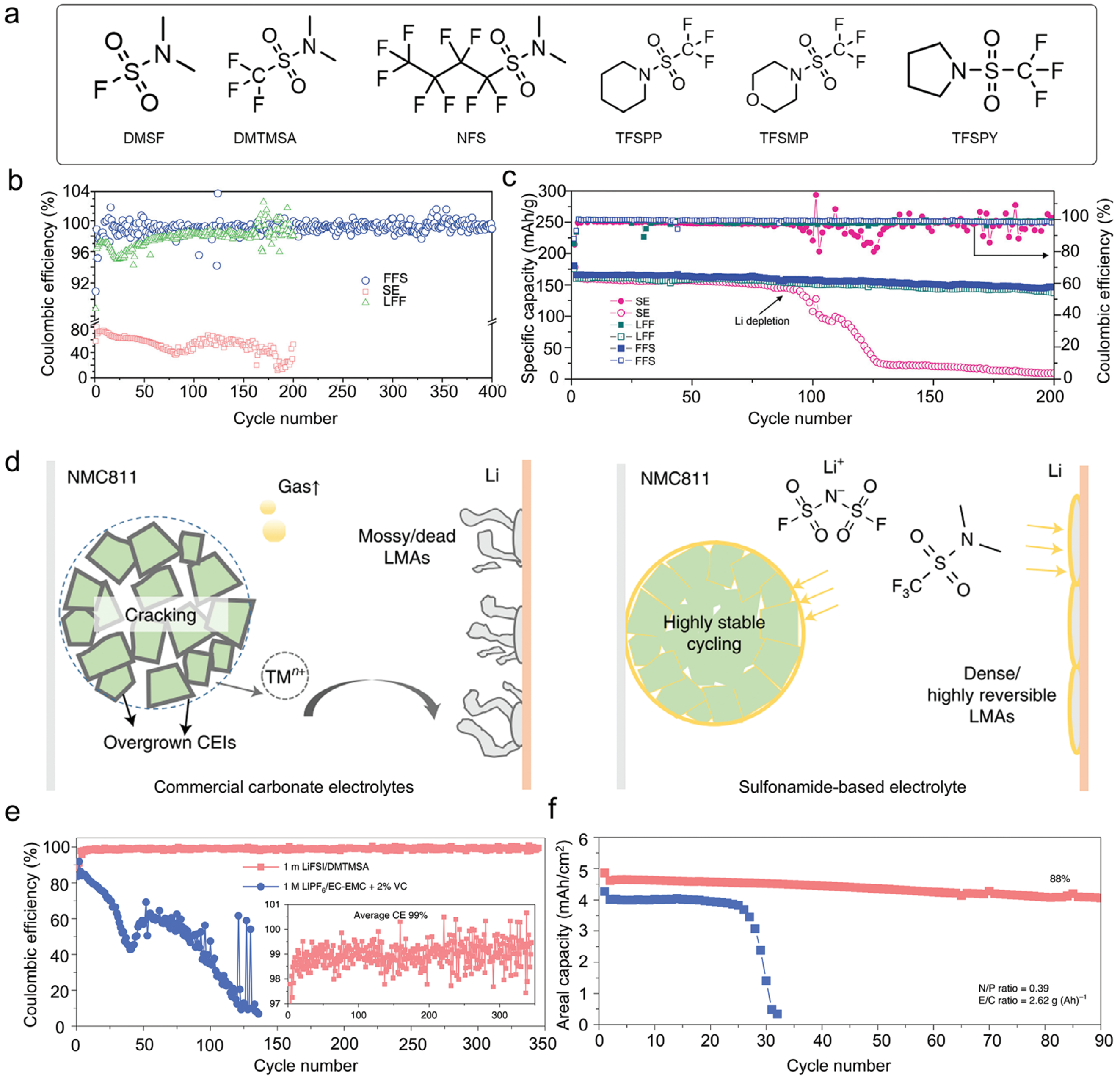

Figure 9. Molecular engineering for new sulfonamides. a) Molecular structures of the sulfonamides. b) Li plating/stripping CEs evaluated by Li||Cu coin cells in the FFS electrolyte. c) Cycling performance of the Li||NMC622 (50-µm-thick Li metal foil) cells in the FFS electrolyte. Reproduced with permission.[137] Copyright 2022, RSC Publishing. d) Inhibit the intergranular cracking of cathode materials and the formation of dense Li deposition in the DMTMSA-based electrolyte. e) Li plating/stripping CEs evaluated by Li||Cu coin cells and f) Electrochemical performance Li||NMC811 cells (>4 mAh cm^{-2}) at 4.7 V cut-off voltage with the 1 m LiFSI/DMTMSA electrolyte (pink) and the 1 M LiPF$_6$ EC-EMC+2% VC electrolyte (blue). Reproduced with permission.[138] Copyright 2021, Nature Publishing Group.

TFMTMS-based electrolyte (0.4 m LiTFSI + 0.4 m LiNO$_3$ in DME/DOL/TFMTMS) can form robust SEI to minimize Li depletion and enable Li–S pouch cells to cycle over 100 cycles with little excess LMA (60 µm) and lean electrolyte (E/C ratio ~ 4.5 g Ah^{-1}) (Figure 10b).[143] Fan's group designed a family of novel siloxane as solvents, such as dimethyldimethoxysilane (DMMS), tetraethyl orthosilicate (TEOS), methyltriethoxysilane (MTES), and dimethyldiethoxysilane (DMES), with better comprehensive electrochemical performance than ethers and esters, which is reflected by their high compatibility to LMA and high oxidation stability to cathodes simultaneously[144] (Figure 10a,c). Among them, the 1.5 M LiFSI in DMMS electrolyte enables a high average Li–metal plating-stripping CE of ≈99.8% (Figure 10d). Fan's group further developed a fluorinated siloxane-based electrolyte (2.2 M LiFSI in 3,3,3-trifluoropropyl methyldimethoxysilane (TFPDS, Figure 10a)), which could enable a highly reversible

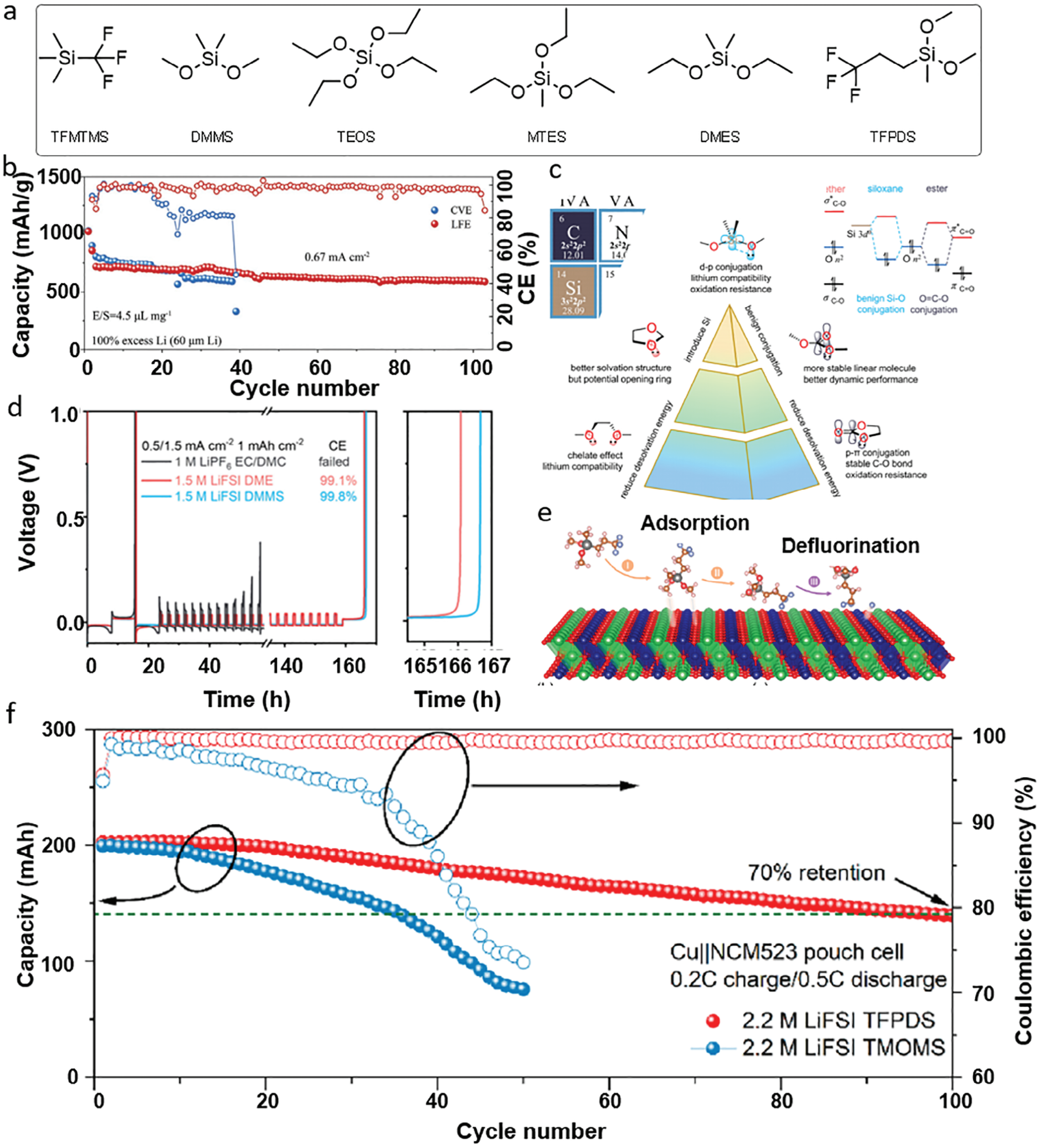

Figure 10. Molecular engineering for silanes. a) Molecular structures of silanes. b) Cycling performance of Li–S pouch cells using 60-μm-ultrathin Li and E/S = 4.5 μL mg^{-1}. Reproduced with permission.[143] Copyright 2021, Wiley-VCH. c) Schematic illustration of the approximated molecular orbitals of ether, siloxane, and ester. d) Modified Aurbach's measurement of the Li metal CE in Li||Cu half-cells using the DMMS-based electrolyte. Reproduced with permission.[144] Copyright 2022, RSC Publishing. e) Schematic illustration of an adsorption–defluorination dynamic process of TFPDS on the cathode. f) Cycling performance of the anode-free Cu||NMC532 pouch cells using the 2.2 M LiFSI/TFPDS and reference electrolytes. Reproduced with permission.[145] Copyright 2023, ACS Publishing.

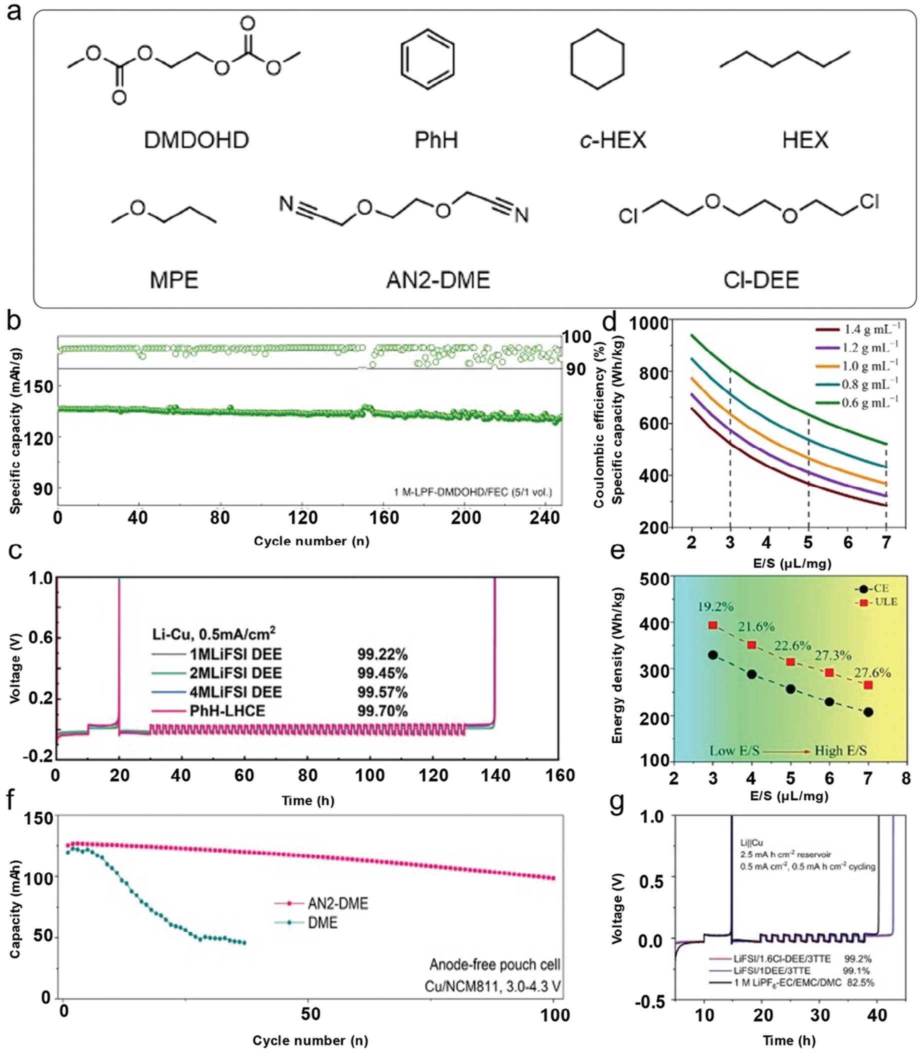

Figure 11. Molecular engineering for Fluorine-free molecules. a) Molecular structures of several fluorine–free solvent molecules. b) Cycling stability of the Li||$LiNi_{0.5}Mn_{1.5}O_4$ cell in 1 M-$LiPF_6$-DMDOHD/FEC electrolyte at a rate of C/3. Reproduced with permission.[151] Copyright 2024, Nature Publishing Group. c) Li-metal plating-stripping CE in the PhH-based LHCE measured by modified Aurbach method at 0.5 mA cm^{-2}. Reproduced with permission.[153] Copyright 2024, Wiley-VCH. d) Relationship between the electrolyte density and the estimated E_g of Li–S full cell. e) The improvement in specific energy of Li–S pouch cells by using the ultralight electrolyte at different E/S ratios. Reproduced with permission.[155] Copyright 2022, Wiley-VCH. f) Electrochemical performance of anode-free Cu||NCM811 pouch cells using the AN2-DME electrolyte. Reproduced with permission.[156] PNAS. g) Li-metal plating-stripping CE at 0.5 mA cm^{-2} with the LiFSI/1.6Cl-DEE/3TTE electrolyte. Reproduced with permission.[157] Copyright 2022, Wiley-VCH.

LMA and simultaneously release the F-atoms to form thin SEI on high-voltage LCO via an adsorption–defluorination process (Figure 10e), exhibiting stable cycling of the 4.5 V Li||LCO cells with 95% capacity retention over 400 cycles.[145] Impressively, with this electrolyte, a highly stable anode-free Cu||NMC532 pouch cell was achieved with 70% capacity retention for 100 cycles (Figure 10f).

4.1.5. Other Fluorine-Free Molecules

From the above discussions, it is notable that the LMA reversibility is greatly affected by the fluorine released from the electrolyte components. In order to describe this relationship, Suo et al. defined a donatable fluorine concentration (DFC) and discovered that the Li–metal plating-stripping Coulombic inefficiency (CIE) (CIE = 1 − CE) decays nearly exponentially with increasing the DFC in the LiFSI-FEC electrolytes.[56] Besides the well-known LiF, recently, Gustavo et al.[146] discovered that the Li metal plating-stripping CE has a strong relationship with Li_2O content in SEI measured by a titration method, revealing the beneficial role of Li_2O. They successfully established a theoretical guidance, which supports the development of high-performance F-free electrolytes for LMBs.[147–150] In this section, we will focus on several fluorine-free solvent molecules for LMB electrolytes (**Figure 11**a).

By rationally designing the molecular structure, Zhang et al.[151] and Dahn's group[152] developed a new dicarbonate molecule, dimethyl 2,5-dioxahexanedioate (DMDOHD), by combining the functional structures of EC, DMC, and EMC. Li metal

CEs have achieved >90% with the 1 M $LiPF_6$ in DMDOHD electrolyte, higher than the cell with the traditional 1 M $LiPF_6$ in EC/DMC electrolyte. More importantly, the DMDOHD-based electrolyte has unique anodic stability to well match a 5-V-class $LiNi_{0.5}Mn_{1.5}O_4$ (LNMO) cathode with excellent capacity retention of >97% after 250 cycles (Figure 11b).[151] Some liquid-state F-free hydrocarbons, featuring their nonpolarity and inertness, have been reported as diluents for developing LHCEs. Li et al. developed low-cost LHCEs using benzene (PhH) as a diluent, achieving an average Li–metal CE of ≈99.7% and highly reversible Li||NMC (83% Ni content, single crystalline) cells at a high cathode loading of 31 mg cm^{-2} and E/C = 4.6 μL mAh^{-1} (Figure 11c).[153] In addition, *n*-hexane (HEX) and cyclohexane (*c*-HEX)[154] can decrease the overpotentials for Li^0 nucleation and growth and improve the Li–metal CE when combined with DME as co-solvent and LiTFSI as salt.

The electrolyte is a main cell component, especially in Li–S batteries with more electrolytes than in traditional LIBs. Suo's group[143,155] proposed a smart way to boost the cell-level E_g. A series of "ultralight" electrolytes with densities of 0.8–1.0 g mL^{-1} (compared to 1.3 g mL^{-1}, 1 M $LiPF_6$ in EC/DMC) were developed, which could theoretically boost the cell-level E_g by 24.4% if E/S ~ 3 μL mg^{-1} (Figure 11d). This was realized by novel LMA-compatible solvent molecules with minimizing or even removing the "heavy" atoms (e.g., F, O) in molecules. As shown in Figure 11e, the electrolyte with a novel monoether (methyl propyl ether, MPE, 0.712 g mL^{-1} at 25 °C, Figure 11a) can enable a Li–S pouch cell with a cell-level E_g of 393.4 Wh kg^{-1}, 19.2% higher than the pouch cell with the conventional electrolyte (329.9 Wh kg^{-1}, 1 M LiTFSI in DME/DOL with 2 wt% $LiNO_3$).[155] Suo's group also designed another successful F-free molecule (ethylene glycol bis(propionitrile) ether, AN2-DME, 1.07 g mL^{-1} at 20 °C, Figure 11a) by introducing an electron-withdrawing group cyanogen into an ether molecule. The AN2-DME-based electrolyte (1 M $LiPF_6$ in AN2-DME/FEC/TTE) can enable Li||Cu cells with an average Li–metal CE of 98.4% over 100 cycles. The anode-free Cu||NMC811 pouch cells with the AN2-DME-based electrolyte can maintain an impressively high capacity retention of 76% after 100 cycles (Figure 11f).[156] Besides these approaches, Ren's group demonstrated a chlorine substitution strategy instead of the fluorine substitution and developed a new ether molecule, 1,2-bis(2-chloroethoxy)-ethyl ether (Cl-DEE, Figure 11a).[157] The Cl-DEE-based electrolyte (LiFSI/Cl-DEE/TTE, 1:1.6:3 molar ratio) achieved a high Li–metal CE of 99.2% (Figure 11g) and very good anodic stability up to 4.7 V vs. Li/Li^+ when matching with the Ni-rich cathode. The intrinsic nonflammability of the Cl-DEE solvent is beneficial to the cell safety.

4.1.6. Fluorinated Hydrocarbon

In 2017, Meng's group proposed a revolutionary liquefied gas electrolytes (LGEs) concept by introducing a series of typical gas molecules (e.g., fluoromethane (FM), difluoromethane (DFM), fluoroethene (FE) **Figure 12a**) as electrolyte solvents via exerting proper pressure in a hermetically sealed cell,[158] which differs from the classic liquid or solid-state electrolytes. These LGEs in a supercritical state feature their wide electrochemical stability window, low viscosity, and good wettability over a wide temperature range from −78 to +65 °C. The FM -based electrolyte (0.2 M LiTFSI in FM: CO_2 = 19:1 wt) showed high Li–metal CE of ≈97% and good cyclability of Li||LCO cells operated as low as −60 °C. To increase the salt concentration and thus the ionic conductivity of the LGEs, they proposed to use an additive-amount of co-solvent (tetrahydrofuran (THF) or acetonitrile (AN)) to dissociate the Li salt (Figure 12b). Together with Li–metal CEs as high as 99.6%, an impressive Li^+ conductivity of the resulting electrolyte (0.3 M LiTFSI + 0.3 M THF in FM: CO_2 = 19:1 wt) at −60 °C (2.8 mS cm^{-1}) was achieved, much higher than the previous LGEs without THF (1.1 mS cm^{-1}).[159] In addition, AN was also used as a co-solvent for LGEs[160] to match the NMC cathode with a cut-off voltage of 4.5 V vs. Li/Li^+ over a wide temperature range of −60 to 55 °C. Besides these gaseous alkanes for LGEs, the simplest ether dimethyl ether (Me_2O) was also discovered as an excellent candidate for LGEs since it has the lowest freezing point and viscosity among all ethers combined with high solvating power, reductive stability, and good compatibility with Li metal. Together with two hydrofluorocarbon molecules, 1,1,1,2-tetrafluoroethane (TFE), pentafluoroethane (PFE) (Figure 12a), the 1 M LiFSI in Me_2O-TFE-PFE (7:1 v) LGE can enable Li^+ conductivity >3 mS cm^{-1} from −78 to 80 °C,[161] Li–metal CE >99% for over 200 cycles at 3 mA cm^{-2} & 3 mAh cm^{-2}, and stable cycling of Li||NMC622 cells from −60 to 55 °C (Figure 12c).

In addition to the above liquefied short-chain hydrofluorocarbons, hydrofluorocarbon molecules with longer chains and more F atoms are liquid under standard conditions. For example, Fan's group developed an LHCE based on 2H, 3H-decafluoropentane (HFC, **Figure** 12a), in which a solvation structure with a higher energy barrier of de-coordination enables practical 4.4 V Li||NMC811 cells with high capacity retention >90% over 180 cycles with an N/P ratio ~1.1.[162] Furthermore, other hydrofluorocarbons have been utilized in LMBs, such as 1,2-difluorobenzene (DFB),[163] (Trifluoromethyl) cyclohexane (FMCH),[164] etc. Most recently, Fan's group developed an FMCH-based LHCE dominated by a unique anion-less solvation structure,[164] restricting the transportation of additional electrons from anions to ether molecules and thus improving the oxidation resistance. Together with the formation of Li_2O and LiF-rich SEI on the LMA, the 4.5 V 30-μm-Li||3.8-mAh cm^{-2}-$LiCoO_2$ battery can maintain 80% capacity retention after 440 cycles (Figure 12d).

In summary, we compared the advantages and disadvantages of different solvents in **Table 1**. Fluorination of carbonates or ethers can improve their compatibility with both the LMA and the high-voltage cathodes with the expense of decreasing the salt solubility and some of them are very sensitive to moisture or residual water in electrolyte. The sulfonamides exhibit superior oxidation stability for high-voltage cathodes with good LMA compatibility while the salt solubility and the Li^+ conductivity of electrolyte are still limited. Due to their low density, silanes are promising solvents for LMBs for improving energy density, but their poor oxidation resistance still hinders their collaboration with high-voltage cathodes. Some fluorine-free solvents are in a similar situation as the silanes although they are more eco-friendly than fluorinated solvents. Fluorinated hydrocarbons can enable dendrite-free Li–metal deposition and high

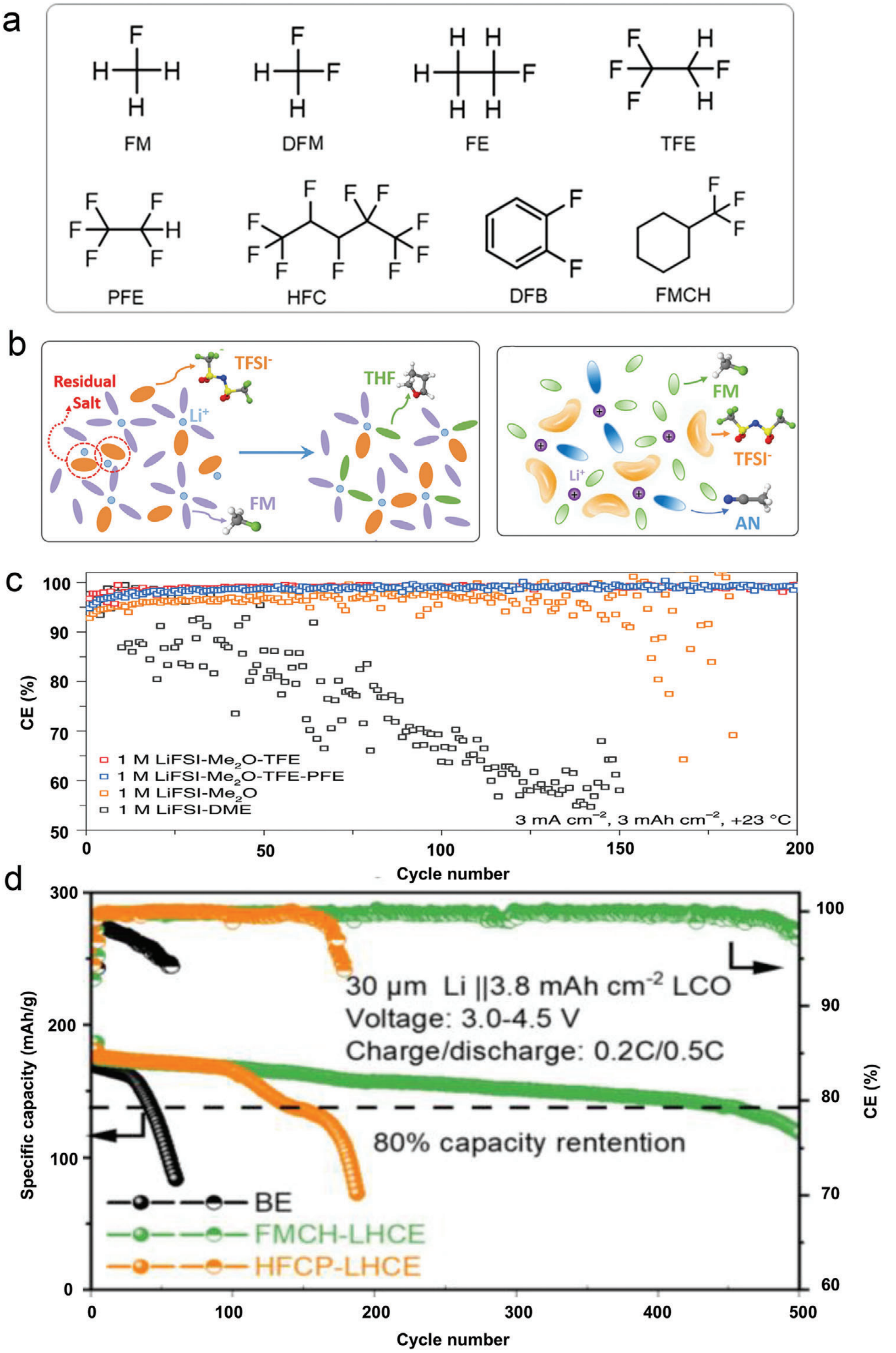

Figure 12. Molecular engineering for fluorinated hydrocarbon molecules. a) Molecular structures of liquefied gas molecules. b) Schematic illustration of the solvation sheath of the LGE with THF or AN. Reproduced with permission.[159] Copyright 2019, Elsevier. Reproduced with permission.[160] Copyright 2020, RSC Publishing. c) Electrochemical performance of the LMAs in the Me_2O-based LGEs. Reproduced with permission.[161] Copyright 2022, Nature Publishing Group. d) Long-term cycling performance of 4.5 V Li||LCO (N/P = 1.45) cells at charge/discharge rate of 0.2 C/0.5 C in the FMCH-LHCE. Reproduced with permission.[164] Copyright 2024 Wiley-VCH.

Table 1. The advantages and disadvantages of different solvents.

Solvents	Advantages	Disadvantages
Fluorinated carbonates	High oxidation resistance	Low salt solubility Poor stability with water
Fluorinated ethers	High LMA compatibility	Limited salt solubility/conductivity
Sulfonamides	High oxidation resistance, High LMA compatibility	Low salt solubility/conductivity
Silanes	Low density	Poor oxidation resistance
Fluorine-free molecules	Low density Environmental-friendly	Low salt solubility
Fluorinated hydrocarbon	Low density High LMA compatibility	Low salt solubility/conductivity High-pressure container required

CE but need to work with high-pressure containers. Therefore, as the most prevailing electrolytes for LIBs, multiple solvents should also be employed for LMBs to balance their advantages and disadvantages, depending on the specific practical application.

4.2. Molecular Engineering for Lithium Salts

Although rationally designing new solvent molecules greatly improves the LMA-compatibility of the electrolyte, LiFSI is still dominant as the main salt in most works (**Figure** 13a). LiFSI is a typical sulfonamide-type salt with a highly conjugated anionic center (–SO_2–N^-–SO_2–) and single F atom at both ends, featuring its high Li^+ conductivity and LMA compatibility. Another prevailing sulfonamide-type salt, LiTFSI (Figure 13a), is commonly used as the main salt for Li–S batteries working together with ethers and $LiNO_3$ to achieve high Li–metal CE and good chemical stability with the LiPS. However, a bottleneck of these sulfonamide-type salts hindering their extensive applications as main salts, is their corrosion to Al current collector at high potentials (e.g., >3.8 V vs Li/Li^+).[165–167] To tackle the Al corrosion issue of LiTFSI, Qiao et al.[168] proposed a smart molecular modification approach to create an asymmetric LiDFTFSI (difluoro methanesulfonyl) (trifluoromethanesulfonyl) imide) salt (Figure 13a). The new LiDFTFSI salt shows remarkable anodic stability against Al corrosion even at high potentials >4.2 V vs. Li/Li^+ by forming $Al(DFTFSI)_3$-derived insoluble products to passivate Al. Benefiting from its good compatibility with the LMA at the same time, LiDFTFSI is considered to be a promising salt for HVLMBs. Inspired by the smallest surface tension (γ) of $-CF_3$ among all $-CH_xF_y$ groups, Cui's group[169] designed an Al-centered, 8-$-CF_3$-surrounded lithium perfluoropinacolatoaluminate (LiFPA) salt (Figure 13a) synthesized by a simple one-step, one-pot method. LiFPA can effectively reduce surface tension and improve the wettability of electrolytes, which promotes the formation of favorable Li deposits with more compact, smooth, and dendrite-free morphology. Practical LMBs with LCO and NMC622 cathodes with good cycling stability were achieved by the LiFPA-based electrolytes.

It is often challenging for fast charging in LMBs because unstable Li^0 electroplating occurs when currents exceed diffusion limitation.[41] Therefore, from the viewpoint of required electrolyte physicochemical properties for fast-charging LMBs, high donor number (DN) and Li^+ transference number ($t_{Li}{}^+$) are essential. In order to realize fast charging, a novel lithium 1,1,1-trifluoro-*N*-[2-[2-(2-methoxyethoxy) ethoxy)] ethyl] methanesulfonamide (LiFEA, Figure 13a) salt was proposed by Liu's group,[170] featuring its asymmetric molecule structure derived from LiTFSI by substituting a trifluoromethanesulfonyl unit with an ethylene glycol group. A pseudo-crown ether-like binding geometry between the salt anion and Li^+ enables a large dipole moment, high DN, and $t_{Li}{}^+$ when LiFEA is used as an additive (≈0.1 M) for the 1 M $LiPF_6$ in EC/DEC (1:1 v) electrolyte. Remarkably, under fast-cycling conditions (charging/discharging: 1.46/3.66 mA cm^{-2}), Li||NMC811 pouch cells with a high cathode loading ~ 3.6 mAh cm^{-2} and lean electrolyte E/C ratio <2.8 g Ah^{-1} maintained 81% capacity after 100 cycles (Figure 13b). They further modified the LiFEA molecule by adding an extra electron-withdrawing sulfonyl group near the N atom, yielding a lithium 2-[2-(2-methoxy ethoxy) ethoxy] ethane sulfonyl(trifluoromethanesulfonic) imide (LiETFSI, Figure 13a) salt.[171] The alteration in the molecular structure enhances ionic dissociation and the proposed SEI self-cleaning mechanism (Figure 13c), resulting in even better fast-charging–discharging capability with LiETFSI as an additive in 1 M $LiPF_6$ in EC/DEC (v/v = 1:1) electrolyte. The advanced LiETFSI-based electrolyte enables Li||NCM811 cells with 40 µm Li foil and high-loading NCM811 to achieve stable cycling over 250 cycles even at a high charging/discharging rate of 2 C (≈4 mA cm^{-2}) (Figure 13d).

In addition, LiDFOB and $LiBF_4$ are usually working synergistically to form protective B-contained robust SEI on the LMA.[172,173] Dahn's group pioneered a series of such dual-salt electrolytes (LiDFOB/$LiBF_4$ in FEC−DEC), enabling an anode-free Cu||NMC532 pouch cell to retain 80% capacity after 90 cycles.[174–176] It is worth noting that LiDFOB and $LiBF_4$ have been used only as additives in LIBs electrolytes, but would play a more important role in LMB electrolytes (e.g. as main salts), demonstrating that LMBs are giving new opportunities for novel salts designed by molecular engineering.

4.3. Molecular Engineering for Additives

Electrolyte additives are always used in a small quantity but are important in altering the SEI/CEI compositions, greatly impacting battery performance. For example, vinylene carbonate (VC) and 1,3,2-dioxathiolane 2,2-dioxide (DTD) are common additives for SEI formation to improve room- and high-temperature cycling performance in LIBs. However, most such useful additives

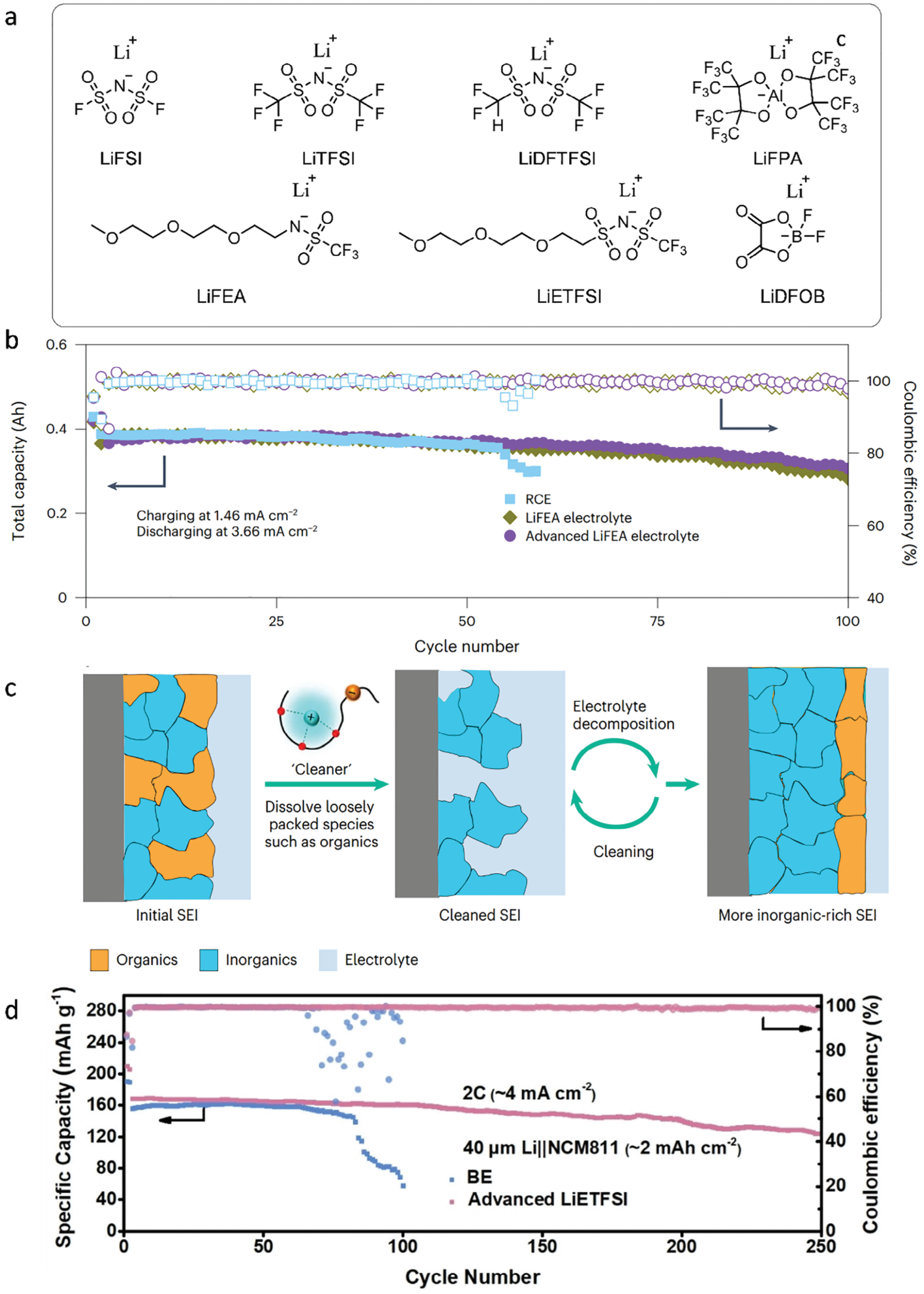

Figure 13. Molecular engineering for lithium salt molecules. a) Molecular structures of lithium salts for LMBs. b) Electrochemical performance of a Li||NCM811 pouch cell (3.66 mAh cm^{-2}, N/P = 2.7, E/C = 2.8 g Ah^{-1}) with the LiFEA-based electrolyte. c) The proposed self-cleaning of the SEI mechanism. Reproduced with permission.[170] Copyright 2023, Nature Publishing Group. d) The cycling performance of Li||NCM811 full cells at 2 C with advanced LiETFSI electrolyte. Reproduced with permission.[171] Copyright 2024, Wiley-VCH.

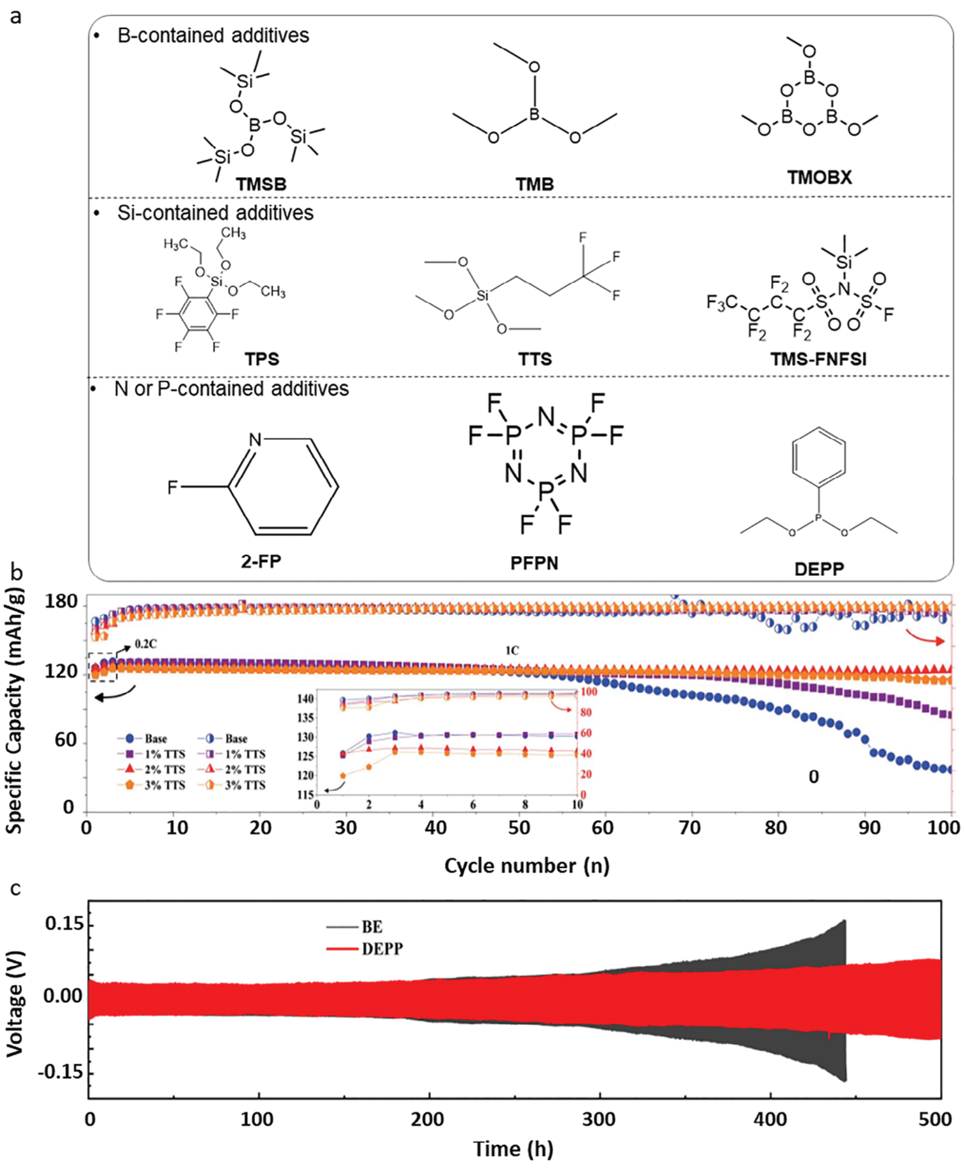

Figure 14. Molecular engineering for additives molecules. a) Molecular structures of additives for the LMBs. b) Cycling stability of high-loading LNMO||Li cells operated in the baseline and TTS-containing electrolytes. Reproduced with permission.[187] Copyright 2020, RSC Publishing. c) Cycling performance of Li||Li cells in the electrolyte with and without 0.1 wt% DEPP. Reproduced with permission.[210] Copyright 2021, Elsevier.

in LIBs are less employed in LMBs mainly due to the different SEI formation and surface chemistry required for the LMA from the graphite anode. Therefore, new additives are particularly designed and developed for LMBs (**Figure 14a**).

1) *Boron-contained additives*: As boron atoms can act as Lewis acid sites to form strong interactions with anions, more anions, and Li^+ cations could be moved into the double electron layer (EDL) near the LMA surface, resulting in favorable and stable inorganic-rich SEI.[177–179] Zhang et al. introduced 1 wt% tris(trimethylsilyl) borate (TMSB) to a carbonate-based electrolyte (1.5 M $LiPF_6$ in FEC/EMC/DMC), which achieved an average Li–metal CE of 97.94% over 500 cycles, compared to the much shorter cycle life (200 cycles) with the electrolyte without TMSB.[180] A 2.5 Ah prototype pouch cell was used to demonstrate the effectiveness of the TMSB additive, reaching a high E_g ≈357 Wh kg^{-1} with 90.90% capacity retention over 50 cycles. In addition to improving the LMA compatibility, B-contained additives tend to form highly Li^+ conductive B–O and B–F species on the cathode surface to protect it from degradation, such as trimethyl borate (TMB),[181,182] trimethoxyboroxine (TMOBX).[183]
2) *Silicon-contained additives*: Silicon (Si)-contained additives are effective in stabilizing the cathode–electrolyte interface by scavenging the harmful and corrosive HF species in the electrolytes.[184] Recent studies discovered that a robust artificial SEI layer with Li–O–Si bonds can improve the air and cycling stability of the LMA.[185] Some Si-contained additives have been reported in LMBs, including poly-ether modified siloxanes,[186] pentafluorophenyltriethoxysilane (TPS),[184]

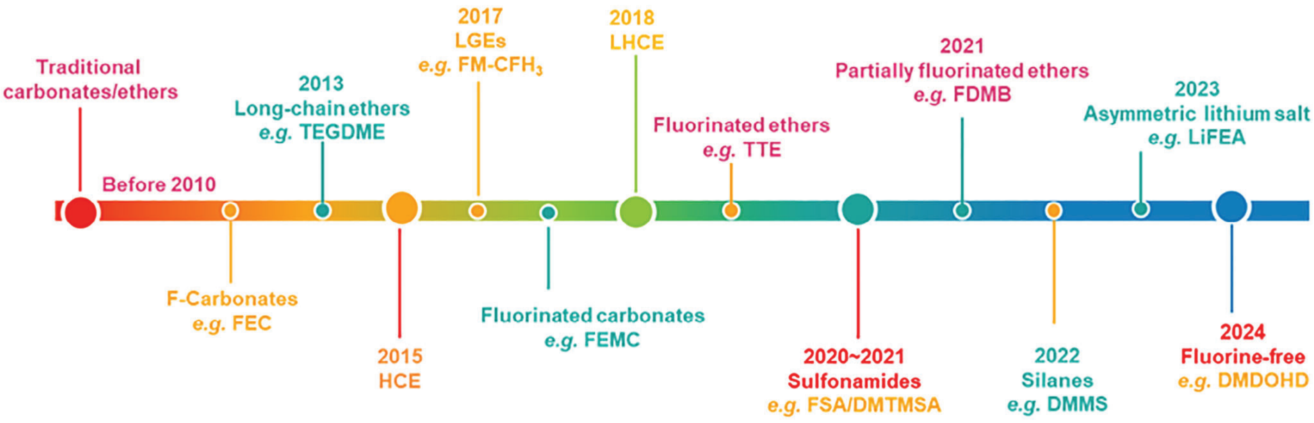

Figure 15. The timeline of electrolyte molecular engineering.

and trimethoxy (3,3,3-trifluoropropyl) silane (TTS).[187] Zhou et al.[188] introduced 5 wt% Si-contained additive trimethylsilyl(fluorosulfonyl) (*n*-nonafluorobutanesulfonyl) imide (TMS-FNFSI) into the 1 M LiTFSI in DOL/DME (1:1 v) electrolyte, showing high Li–metal CEs >96.5%. Furthermore, Chen et al.[187] discovered that TTS helps create protective films on both the LMA and high-voltage cathodes, while also scavenging harmful HF by Si–O groups. Impressively, the capacity retention of the Li||LNMO cell with 2% TTS additive is much higher (97%) than the blank electrolyte without TTS (28%) over 100 cycles (Figure 14b).

3) *Nitrogen-contained additives*: The most prevailing N-contained additive for LMBs is $LiNO_3$,[189–192] which was first discovered for Li–S batteries. It can be reduced on the LMA surface at a higher potential than the LiPS does, protecting the LMA from LiPS corrosion and greatly prolonging the cycle life of Li–S batteries.[193–199] Other nitrates with different cations such as $CuNO_3$,[200] $CsNO_3$,[201] $RbNO_3$[202] have also been explored. Hu et al. demonstrated that large Cs^+ has weaker interaction with solvent molecules than Li^+, leading to the presence of anions in the solvation sheath and anion-derived interphase.[201,203] Interestingly, the resultant CsFSI-derived SEI endowed higher Li–metal CE (99.46%) than the blank electrolyte without $CsNO_3$ (99.1%). 2-fluoropyridine (2-FP) with a pyridine ring was reported to be an effective additive in the 1 M $LiPF_6$ in EC/DEC (1:1 v) electrolyte.[204] The presence of only 2 wt% 2-FP can promote the formation of stable and robust SEI with LiF and Li_3N components, thus exhibiting higher Li–metal CE ~ 90.61% after 50 cycles than the blank electrolyte without 2-FP (49.59%).
4) *Phosphorus-contained additives*: Phosphorus-based compounds are typically used as flame-retardant additives in LIBs due to their ability to capture radicals.[205,206] Some P-contained additives are also reported to form favorable SEI components on the LMA. Wu's group[207] revealed that ethoxy(pentafluoro)cyclotriphosphazene (PFPN) can work as a multifunctional additive to protect both the LMA and high-voltage cathodes (LCO and LNMO). After adding 10% PFPN into the 1 M $LiPF_6$ in EC/DEC (1:1 v) electrolyte, the 5-V-class Li||LNMO cells exhibited a much higher capacity retention of 90.7% over 100 cycles, than the one with the PFPN-free electrolyte (47.5%). PFPN can also be employed as solvents/diluents in LHCEs for HVLMBs.[208,209] Furthermore, Miao et al.[210] found that only 0.1 wt% diethyl phenylphosphonite (DEPP) in the 1 M $LiPF_6$/EC/DMC (1:1 v) electrolyte can enable the Li||Li symmetric cell to maintain stable cycling for 500 h, while that with the blank electrolyte started to be polarized after 300 h (Figure 14c).

Here, we encapsulate various cutting-edge molecules that are emerging in the LMBs electrolytes in a timeline (**Figure** 15). We believe that these advanced liquid electrolytes are promising for the deployment of viable LMBs in the future.

5. Electrolyte Design for Extreme Conditions

Besides the most important parameters (e.g. energy density and cycle life), the practical LMBs need to fulfill other requirements under extreme conditions like low/high temperatures, fast charging, and heat abuse, which largely depends on the physicochemical properties, chemical stability, and flammability of electrolyte. Here, we review the guidelines for designing LMB electrolytes under such circumstances as below.

5.1. Low-Temperature Electrolytes

Electrolytes for low-temperature applications should satisfy the following two requirements: a) a low melting point guaranteeing sufficient Li^+ transport and b) weak Li^+–solvent binding to lower the desolvation barrier and thus the cell polarization (**Figure** 16a). Due to its low freezing point (−108.4 °C) and high reduction resistance, tetrahydrofuran (THF)-based LHCEs achieved high CE of ≈99.63% at −30 °C.[211] Solvents with weak solvation capability like DFEC,[87] DMM,[99] and DFM,[160] are also promising electrolyte candidates for low-temperature applications of the LMBs.

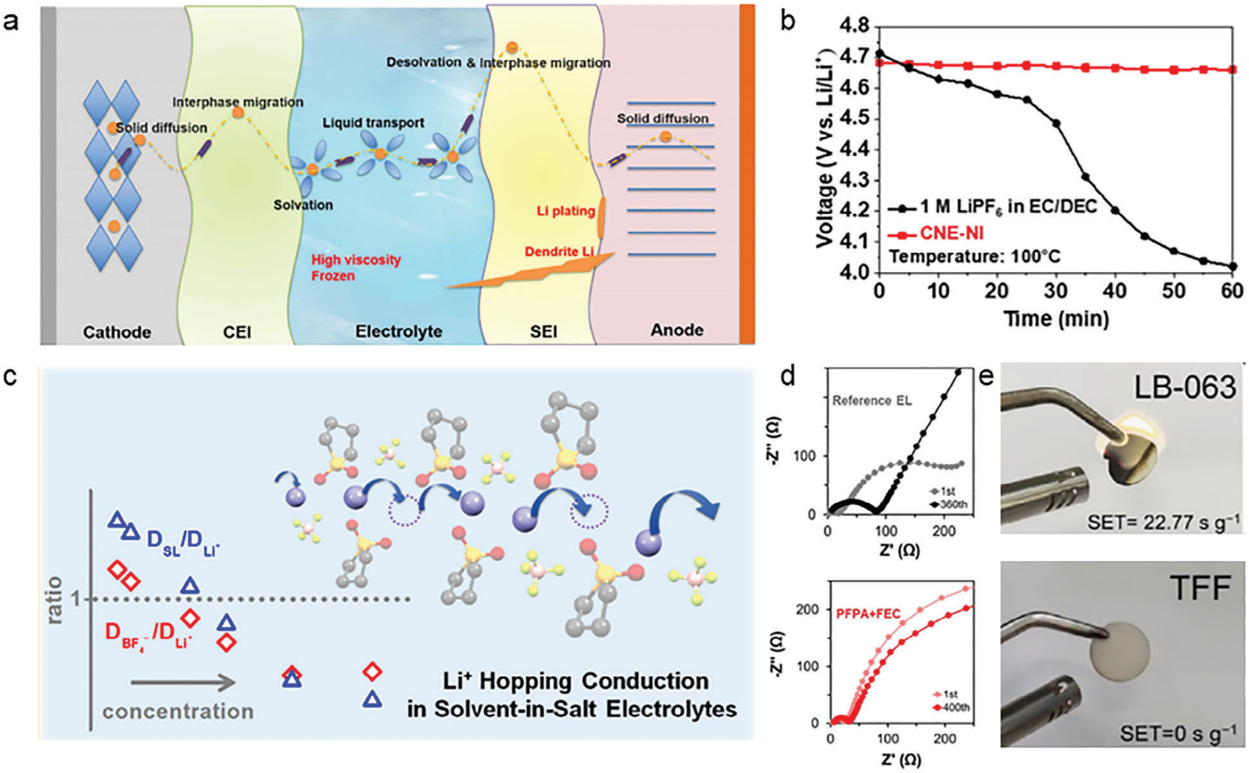

Figure 16. Requirements for electrolytes under different working conditions. a) Schematic diagram of the charging process for the LIB at low temperature. Reproduced with permission.[217] Copyright 2022, Elsevier. b) Open-circuit voltage (OCV) profiles of the Li||LNMO cells with the SN-based electrolyte at 100 °C. Reproduced with permission.[214] Copyright 2022. Wiley-VCH. c) The Li^+ hopping diffusion mechanism in a sulfolane-based HCE. Reproduced with permission.[218] Copyright 2018, ACS Publishing. d) The AC impedance spectral evolution of Li||Mn-rich cells under 20 C with the PFPA-based electrolyte. Reproduced with permission.[216] Copyright 2023, Wiley-VCH. e) The self-extinguish test using 1.5 M LiFSI in TEP: FEMC (1:3 v) and 10 vol% FEC. Reproduced with permission.[60] Copyright 2024, Elsevier.

5.2. High-Temperature Electrolytes

The requirements for electrolytes for high-temperature applications: a) solvents need to possess a high boiling point to avoid gassing at high temperatures and b) the SEI/CEI should be stable at high temperatures to suppress side reactions. LiDFOB is usually used to improve the stability of CEIs at high temperatures.[212] Solvents containing Si or N exhibit excellent thermal stability, such as polymethylsilane[213] and succinonitrile (SN)[214] (Figure 16b).

5.3. Fast-Charging Electrolytes

Electrolytes for fast-charging applications should satisfy the following two requirements: a) high ionic conductivity and Li^+ transference number (Figure 16c) and b) weak Li^+–solvent binding or forming highly conductive SEI/CEI on electrodes. Compared to $LiPF_6$, fluorinated sulfonamide salts (e.g., LiFSI) show excellent ionic conductivity due to higher dissociation in organic solvents. Thanks to the fast Li^+ desolvation in a weakly-solvated FEC and 1,2-difluorobenzene (2FB)-based electrolyte, the Li||NCM811 can retain 77.1% of the original capacity at 5.0 C.[215] Furthermore, the formation of highly conductive SEI on the LMA is also beneficial to fast charging. For example, An et al. reported an electrolyte with co-additives of pentafluoropropionic anhydride (PFPA) and FEC (Figure 16d),[216] which enables ultrafast charging of 20 C in Li||Mn-rich LMBs.

5.4. Nonflammable Electrolytes

Solvents, which can limit or eliminate the generation of free radicals, are key for nonflammable electrolytes. Phosphate esters are widely studied as flame-retardant electrolytes, such as triethyl phosphate (TEP) and trimethyl phosphate (TMP (Figure 16e). Deng et al. designed an ether-based electrolyte with chlorine functionality on a DEE molecule (Cl-DEE) to improve flame-retardant properties.[157]

6. Prospects for the Practical Applications of New Electrolytes in LMBs

In 2017, we pointed out the important role of practical battery conditions in reaching high cell-level energy densities by calculating the full-cell E_g and volumetric energy densities (E_v).[16] Although a lot of progress has been made on LMBs, we believe, especially for electrolyte development, there are still some important perspectives for practical solutions, which could also lead to more interesting scientific research.[219]

6.1. Practical Cell Conditions

The core of practical conditions is to minimize the amount of inactive components including the carbon black, electrode porosity, electrolyte, and excess LMA to maximize E_g and E_v. They are also crucial for studying the real cell failure mechanism. For example, the amount of Li moving per cycle using a high-loading cathode (≈4 mAh cm^{-2}) is one order magnitude higher than the one using a low-loading cathode (≈0.4 mAh cm^{-2}). In such circumstances, the amount of SEI consuming both the LMA and electrolyte is considerable. The exhaustion of either the LMA or the electrolyte and the overpotential growth due to excessive SEI formation could lead to cell failure.

6.2. Accurate Evaluation of Li–Metal CE

Coin cells with a Li||Cu configuration are often used for evaluating the Li-metal CE for a specific electrolyte. To exclude the effect of the surface roughness and treatment conditions of the matrix, another useful method was proposed[220] for measuring the "intrinsic" CE. However, the correlation between high CEs in coin cells and long cycle life in pouch LMBs may not be sufficiently strong. Therefore, "anode-free" coin cells with a Cu||cathode configuration under practical conditions and preferentially "anode-free" pouch cells are strongly recommended for further evaluation of Li-metal CE for electrolytes.

6.3. Large-Format Multilayer Pouch Cells

Due to its low density, the LMA accounts for only 5.5 wt% total weight of the LMB pouch cell (**Figure 17a**). To reach a high E_g, on one hand, it is important to reduce the electrolyte amount, for example, E/C ratio ~ 2.4 g Ah^{-1} (Figure 17b). On the other hand, it is also effective to use cathode materials with high capacity (Figure 17b), for example, high-voltage high-Ni NCM (220 mAh g^{-1}) or Li-rich manganese-based cathodes (252 mAh g^{-1}). By pushing these cell parameters to their limits, the E_g is expected to achieve >550 Wh kg^{-1} (Figure 17b).

In the past decades, lots of scientists and companies have been focused on boosting the E_g of the LMB pouch cells (Figure 17c). So far, the reported E_g values are around 300–510 Wh kg^{-1} with different cycle life. More recently, Jie et al.[221] (Figure 17d) and Fan's group[222] achieved stable cycling of 505.9 Wh kg^{-1} (130 cycles with 91% capacity retention) and 500 Wh kg^{-1} Li–metal pouch cells (150 cycles with 92% capacity retention), respectively. From the viewpoint of reaching higher energy density, anode-free cells (Figure 17e) are lighter and smaller than the ones using the actual LMA. A famous example of the anode-free pouch cells was reported by Dahn's group enabled by the dual-salt electrolyte and high stacking pressure.[174] Yu et al. also reported an anode-free pouch cell achieving an E_g of ≈325 Wh kg^{-1} with 80% capacity retention after 100 cycles.[112] A higher E_g of 442.5 Wh kg^{-1} anode-free pouch cell with a cycle life of 100 cycles was achieved by Suo's group.[88]

For industry, large-format LMB cells with high energy density and more balanced performance (e.g. cycle life, power capability, and scalability) are announced. Solid Energy Systems (SES) Co. Ltd announced their 4-Ah-level LMB pouch cell with 375 Wh kg^{-1} (Figure 17c) (700 Wh L^{-1}) and 700 cycles[223] when charging–discharging at C/5 and 1 C at room temperature, respectively. A higher energy density of 399 Wh kg^{-1} can be reached by constructing a 105.8 Ah pouch cell. Numerous leading companies, for example, CATL, EVE Energy Co., Ltd, Zhejiang Jinyu New Energy Technology Co., Ltd, and Montavista Energy Technologies Corporation, are pursuing the large-scale manufacturing of LMBs with higher energy densities.

Despite the promising high energy density of the LMBs, we have to pay more attention to their volumetric energy density (E_v), especially after long cycles. At a long-term scale, the dense LMA before cycling will become mossy lithium, containing a lot more porosity, dendrites, and trapped gas products and electrolytes. Although it does not affect the E_g, the cell swelling is inevitable (Figure 17f), causing E_v much lower than expected (even lower than the cells with the graphite anode).

6.4. Gassing Issue

Since pouch cells always have much less dead volume than coin cells, gassing-induced fast capacity decay is one of the common reasons for cell failure, especially when operating at high temperatures.[231–234] With lots of gas, the multilayer-assembled electrodes cannot be tightly attached. Although "hard-constrained" cell-formats like cylindrical cells can endure higher internal gas pressure, continuous gas generation is still harmful.[235,236] Therefore, pouch cells are much preferable to coin cells for the evaluation of the gassing issue for electrolytes.

6.5. Practical Operation Conditions

Cycling and storage performance at 45 °C or higher are generally required. Sometimes, storage performance at 60 °C or above at a fully charged state is also important. In this scenario, electrolytes composed of solvents with low boiling points (e.g., <80 °C or even <100 °C) would be problematic. Moreover, the side reactions between the electrolyte and highly reactive LMA/cathodes at high temperatures are more serious than at room temperature. Besides these high-temperature requirements, the charging–discharging capability of LMBs at low temperatures (e.g., below −20 °C) is often required. Therefore, multiple solvents/salts/additives need to be balanced to fulfill these requirements.

6.6. Cost

The large manufacturing of LIBs has been optimized for many years, and the cost of all battery components has been greatly reduced. Nowadays, the price of common carbonates (EC, EMC, DMC, DEC, etc.) is as low as ≈\$1000/ton (as of May 2024). FEC and LiFSI, prevailing in LMB electrolytes, typically used as additives (<2 wt%) in most LIBs, however, are more expensive (\$10 000–20 000/ton). Therefore, considering that electrolyte accounts for 15–20% cost of a cell, the new, but expensive components might be less competitive for commercialization especially

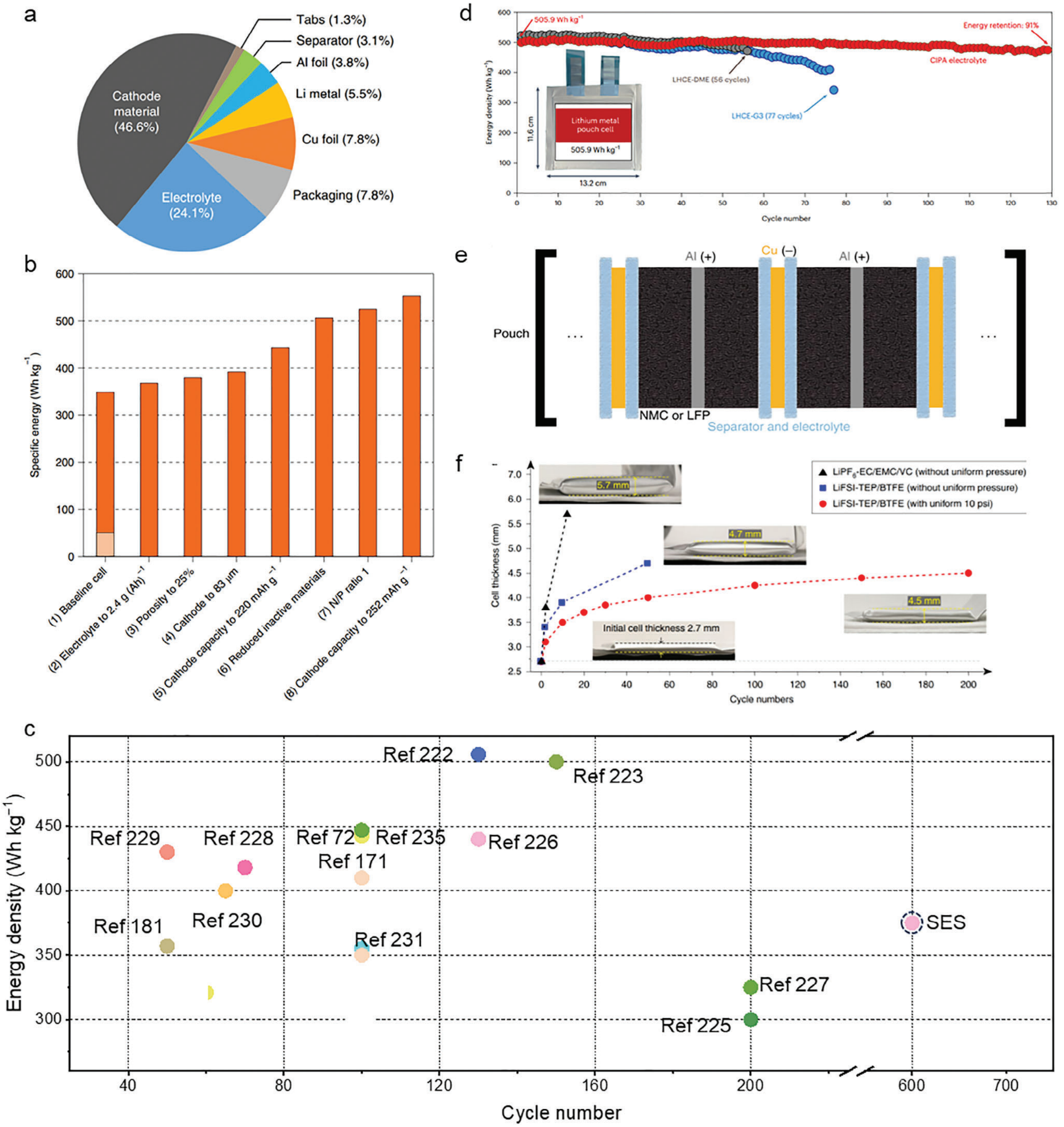

Figure 17. The progress on Li–metal pouch cells. a) A pie chart of the weight distributions of all cell components in LMB pouch cells. Reproduced with permission.[224] Copyright 2019, Nature Publishing Group. b) Calculated cell-level E_g as a function of cell parameters. Reproduced with permission.[219] Copyright 2019, Nature Publishing Group. c) The progress on the E_g of LMB pouch cells.[72,170,180,221,222,224–230] d) Long-term cycling performance of >500 Wh kg^{-1} Li metal pouch cells. Reproduced with permission.[221] Copyright 2024, Nature Publishing Group. e) Cell architecture of anode-free pouch cell. Reproduced with permission.[113] Copyright 2022, Nature Publishing Group. f) The swelling comparison of three parallel Li||NMC622 pouch cells under different conditions with the same initial thickness. Reproduced with permission.[224] Copyright 2019, Nature Publishing Group. E.[72,170,180,221,222,224–230]

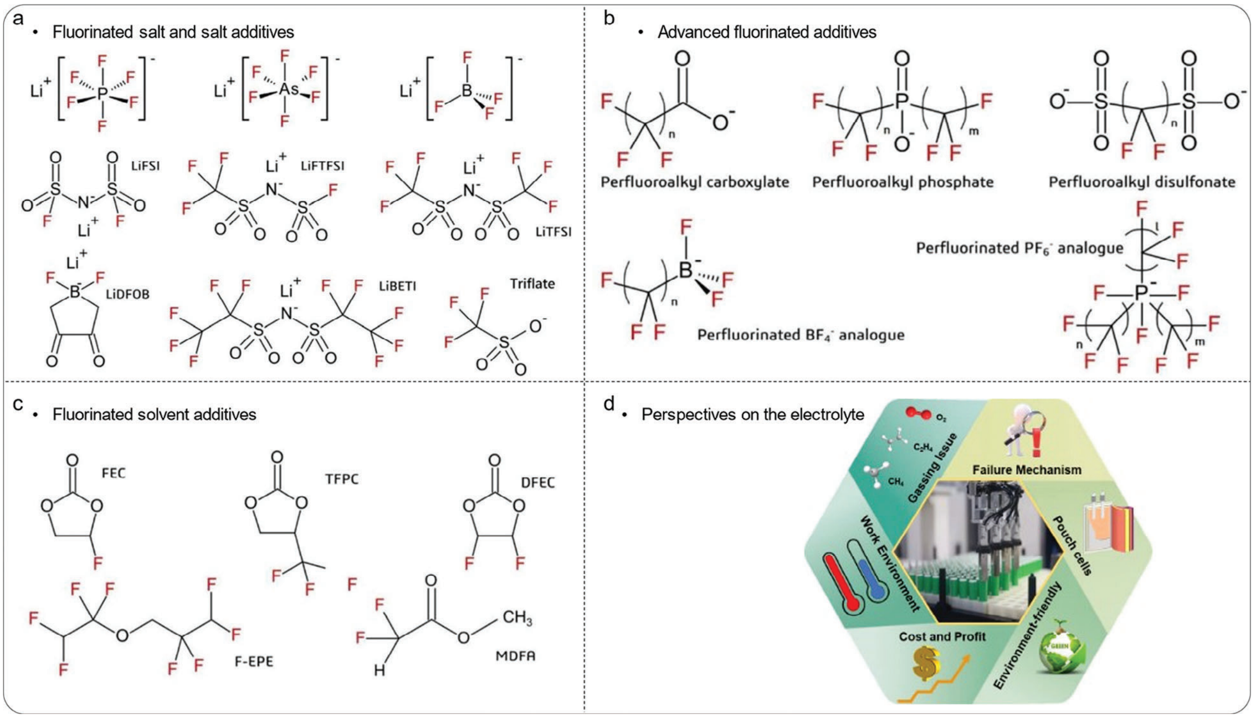

Figure 18. Examples of fluorinated substances found in LMBs components. a) Fluorinated salts, b) advanced fluorinated salt additives, and c) fluorinated solvent additives in LMBs components. Reproduced with permission.[238] Copyright 2023, RSC Publishing. d) Perspectives on the future electrolyte development for LMBs.

when used as the main solvent or salt. The development of low-cost synthesis routes[237] and raw materials are important for new molecules.

6.7. Environmental Impacts

While it is well-known that fluorinated substances (**Figure 18**)[238] are widely used in LIBs, an increasing number may be used in LMBs according to the above discussions. $LiPF_6$, for example, is easily decomposed into $PO_2F_2^-$, HPO_3, POF_3, PF_5, and HF, which are toxic and corrosive.[238] The more troublesome substances are polyfluoroalkyl substances (PFAS), a large class of synthetic chemicals with carbon-fluorine bonds, that are strong chemical bonds against degradation. Concerns have been raised as some of them are increasingly detected as environmental pollutants and potential threats to human health. In January 2023, authorities in Denmark, Germany, the Netherlands, Norway, and Sweden submitted a proposal for restricting ~10000 PFAS to the European Chemicals Agency (ECHA).[239] Therefore, there are plenty of opportunities for the development of fluorine-free electrolyte components, which is important not only for fundamental research but also for mitigating their environmental impacts.

6.8. Artificial Intelligence (AI) Accelerating the Electrolyte Discovery

The discovery of new electrolytes based on molecular engineering usually requires two steps: the discovery of both new molecules and new recipes, which are time-consuming. The discovery of new molecules includes the synthesis, purification, the evaluation of physicochemical properties and electrochemical performance. The design of new recipes also needs extensive investigation of the optimal compositions, which often hides in an immense high-dimensional design space. Conventional human-centered research often requires many repeated and laborious attempts.

Automated flow chemistry[240] that incorporates robotics and active learning algorithms is efficient, speedy, and cost-effective, which is quite suitable for the high-throughput synthesis of new molecules (**Figure 19**a).[241] For example, Mo et al. innovated an electrochemical reactor that operates on microfluidics, enabling the execution of redox neutral electrochemical reactions and fostering the growth of green chemistry (Figure 19b).[242,243] Therefore, the ongoing advancement of automated synthesis offers the potential to create safer, faster, and simpler synthetic protocols for processes that previously depends on manual intervention.

To accelerate the electrolyte recipe design, an artificial intelligence (AI) or machine learning (ML)-assisted platform could integrate high-throughput computational screening and online machine learning.[244] Multiple simulation methods including the DFT and molecular dynamics calculations can be performed to predict the physicochemical properties and the solvation structures, while filtering out the materials design space that is unlikely to present the desired properties.[245,246] Kim et al. developed an ML model capable of predicting and optimizing CE by using a dataset covering a wide design space (Figure 19c)[246] Zhang's group constructed a large database of 1399 solvent molecules by using a graph theory-based

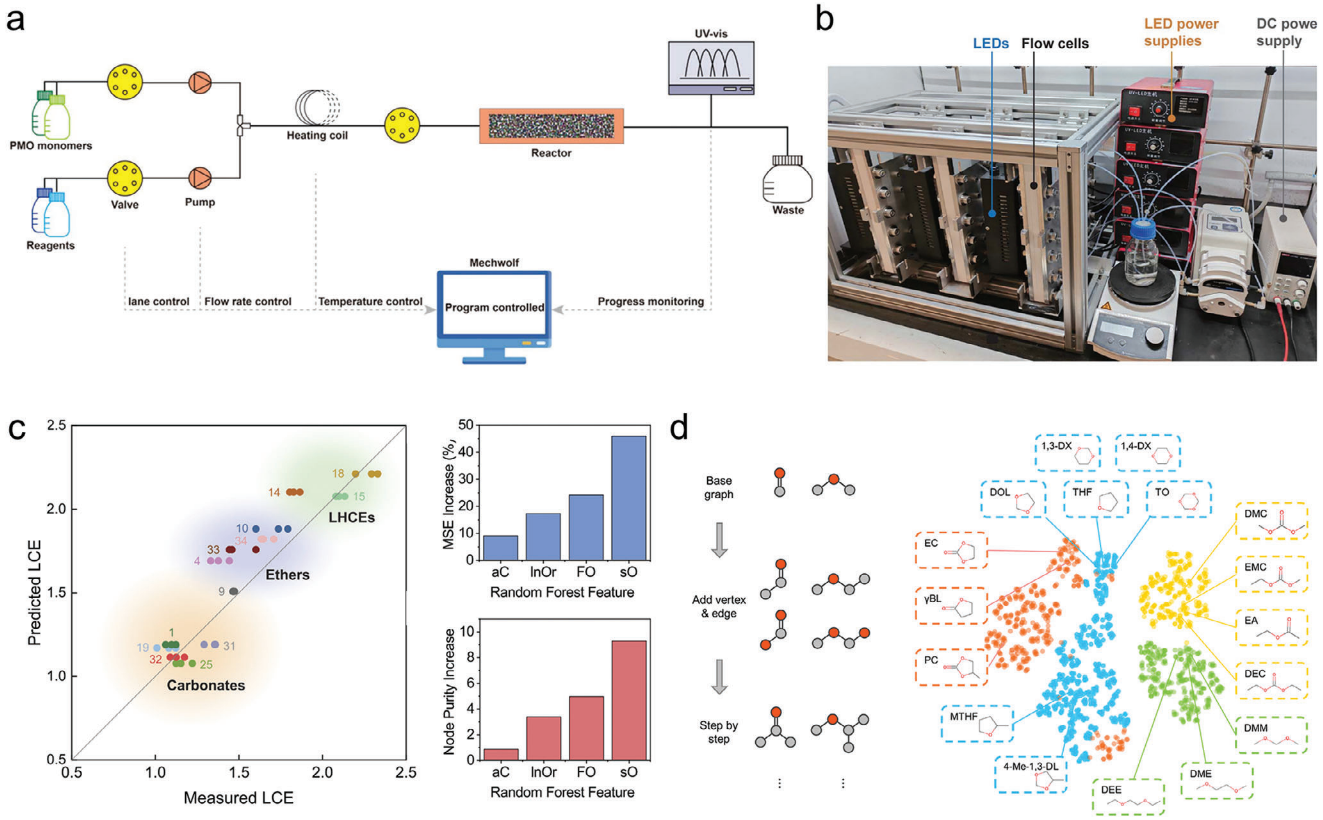

Figure 19. AI and ML expedit the discovery of new electrolyte molecules and recipes. a) Schematic diagram and b) equipment diagram of the high-throughput synthetic compound. Reproduced with permission.[241] Copyright 2023, Nature Publishing Group. Reproduced with permission.[242] Copyright 2024, Science. c) Evaluating the CE of electrolytes under simulated training conditions vs experimentally measured efficiencies. Reproduced with permission.[246] Copyright 2023, PNAS. d) Generation and visualization of the solvent molecular database. Reproduced with permission.[247] Copyright 2023, ACS publications.

algorithm[247] (Figure 19d). By incorporating the ML, we can not only improve the theoretical framework for advanced electrolytes but also revolutionize the design process for next-generation LMBs.

7. Summary

This review presents the most recent advancements in LMBs electrolytes, especially from the viewpoint of molecular engineering, which offers insights into electrolyte design for high-performance LMBs. We summarized the most recent new molecules that are emerging, including new molecules of solvents, salts, additives, and their characteristics and requirements for extreme conditions. The progress from both the academia and the industry on the energy density of high-performance LMB pouch cells was also involved. Some important prospects for developing new electrolytes for practical large-format LMBs in the future are also presented, aiming to push LMBs into practical applications.

Conflict of Interest

The authors declare no conflict of interest.

Keywords

electrolytes, high-voltage cathodes, lithium-metal batteries, molecular engineering

Received: May 31, 2024
Revised: September 6, 2024
Published online:

---

[1] P. Li, G. Zhao, X. Zheng, X. Xu, C. Yao, W. Sun, S. X. Dou, *Energy Storage Mater.* **2018**, *15*, 422.
[2] Z. Li, W. Tang, Y. Yang, G. Lai, Z. Lin, H. Xiao, J. Qiu, X. Wei, S. Wu, Z. Lin, *Adv. Funct. Mater.* **2022**, *32*, 2206615.
[3] C. Zhao, Z. Yang, X. Zhou, Z. Hao, J. Chen, Z. Wang, X. Chen, X. Wu, L. Li, L. Li, L. Jiao, S. Chou, *Adv. Funct. Mater.* **2024**, *34*, 2303457.
[4] R. Kan, M. Jiang, K. Song, R. Chen, Q. Shen, R. Wang, G. Weng, B. Fu, C. Song, P. Tao, J. Wang, M. D. Dickey, T. Deng, W. Shang, *Adv. Funct. Mater.* **2023**, *34*, 2309861.
[5] G. He, X. Han, R. Zou, T. Zhao, Z. Weng, S. Ho-Kimura, Y. Lu, H. Wang, Z. X. Guo, I. P. Parkin, *Adv. Funct. Mater.* **2017**, *27*, 1604903.
[6] Y. Li, Q. Qu, L. Lv, J. Shao, H. Zheng, *Adv. Funct. Mater.* **2024**, *34*, 2314100.
[7] H. Zhang, X. Liao, Y. Guan, Y. Xiang, M. Li, W. Zhang, X. Zhu, H. Ming, L. Lu, J. Qiu, Y. Huang, G. Cao, Y. Yang, L. Mai, Y. Zhao, H. Zhang, *Nat. Commun.* **2018**, *9*, 3729.

[8] D. Lin, Y. Liu, Y. Cui, *Nat. Nanotechnol.* **2017**, *12*, 194.

[9] Y. Xiang, M. Tao, X. Chen, P. Shan, D. Zhao, J. Wu, M. Lin, X. Liu, H. He, W. Zhao, Y. Hu, J. Chen, Y. Wang, Y. Yang, *Nat. Commun.* **2023**, *14*, 177.

[10] L. Lin, K. Qin, Y. S. Hu, H. Li, X. Huang, L. Suo, L. Chen, *Adv. Mater.* **2022**, *34*, 2110323.

[11] X. Tong, X. Ou, N. Wu, H. Wang, J. Li, Y. Tang, *Adv. Energy Mater.* **2021**, *11*, 2100151.

[12] Q. Li, Y. Yang, X. Yu, H. Li, *Chin. Phys. Lett.* **2023**, *40*, 048201.

[13] G. M. Hobold, J. Lopez, R. Guo, N. Minafra, A. Banerjee, Y. Shirley Meng, Y. Shao-Horn, B. M. Gallant, *Nat. Energy* **2021**, *6*, 951.

[14] X. Cao, X. Ren, L. Zou, M. H. Engelhard, W. Huang, H. Wang, B. E. Matthews, H. Lee, C. Niu, B. W. Arey, Y. Cui, C. Wang, J. Xiao, J. Liu, W. Xu, J.-G. Zhang, *Nat. Energy* **2019**, *4*, 796.

[15] W. Xue, Z. Shi, L. Suo, C. Wang, Z. Wang, H. Wang, K. P. So, A. Maurano, D. Yu, Y. Chen, L. Qie, Z. Zhu, G. Xu, J. Kong, J. Li, *Nat. Energy* **2019**, *4*, 374.

[16] W. Xue, L. Miao, L. Qie, C. Wang, S. Li, J. Wang, J. Li, *Curr. Opin. Electrochem.* **2017**, *6*, 92.

[17] Y. S. Jung, A. S. Cavanagh, L. A. Riley, S.-H. Kang, A. C. Dillon, M. D. Groner, S. M. George, S.-H. Lee, *Adv. Mater.* **2010**, *22*, 2172.

[18] A. C. Kozen, C.-F. Lin, A. J. Pearse, M. A. Schroeder, X. Han, L. Hu, S.-B. Lee, G. W. Rubloff, M. Noked, *ACS Nano* **2015**, *9*, 5884.

[19] X. Xiao, P. Lu, D. Ahn, *Adv. Mater.* **2011**, *23*, 3911.

[20] J. Ko, Y. S. Yoon, *J. Korean Ceram. Soc.* **2023**, *60*, 591.

[21] Q. Zhao, X. Liu, S. Stalin, K. Khan, L. A. Archer, *Nat. Energy* **2019**, *4*, 365.

[22] Y. Gao, T. Rojas, K. Wang, S. Liu, D. Wang, T. Chen, H. Wang, A. T. Ngo, D. Wang, *Nat. Energy* **2020**, *5*, 534.

[23] Y. Gao, Z. Yan, J. L. Gray, X. He, D. Wang, T. Chen, Q. Huang, Y. C. Li, H. Wang, S. H. Kim, T. E. Mallouk, D. Wang, *Nat. Mater.* **2019**, *18*, 384.

[24] M. D. Tikekar, S. Choudhury, Z. Tu, L. A. Archer, *Nat. Energy* **2016**, *1*, 16114.

[25] Z. Wang, S. Qin, F. Chen, S. Chen, D. Liu, D. Jiang, P. Zhang, P. Mota-Santiago, D. Hegh, P. Lynch, A. S. Alotabi, G. G. Andersson, P. C. Howlett, M. Forsyth, W. Lei, J. M. Razal, *ACS Nano* **2024**, *18*, 3531.

[26] C. Zhang, A. Wang, J. Zhang, X. Guan, W. Tang, J. Luo, *Adv. Energy Mater.* **2018**, *8*, 1802833.

[27] D. Zhang, S. Wang, B. Li, Y. Gong, S. Yang, *Adv. Mater.* **2019**, *31*, 1901820.

[28] X. Chen, M. Shang, J. Niu, *Nano Lett.* **2020**, *20*, 2639.

[29] M. Bai, K. Xie, K. Yuan, K. Zhang, N. Li, C. Shen, Y. Lai, R. Vajtai, P. Ajayan, B. Wei, *Adv. Mater.* **2018**, *30*, 1801213.

[30] G. Li, Z. Liu, Q. Huang, Y. Gao, M. Regula, D. Wang, L.-Q. Chen, D. Wang, *Nat. Energy* **2018**, *3*, 1076.

[31] Q. Li, S. Zhu, Y. Lu, *Adv. Funct. Mater.* **2017**, *27*, 1606422.

[32] H. Xiao, Y. J. Li, R. Q. Chen, T. C. Xie, P. Xu, H. J. Zhu, J. L. He, W. T. Zheng, S. M. Huang, *eScience* **2023**, *3*, 100134.

[33] T. Li, X.-Q. Zhang, P. Shi, Q. Zhang, *Joule* **2019**, *3*, 2647.

[34] Y. Wu, C. Wang, C. Wang, Y. Zhang, J. Liu, Y. Jin, H. Wang, Q. Zhang, *Mater. Horiz.* **2024**, *11*, 388.

[35] Y. Wang, X. Yang, Z. J. Zhang, X. Hu, Y. F. Meng, X. Wang, D. Zhou, H. Liu, B. H. Li, G. X. Wang, *eScience* **2022**, *2*, 573.

[36] J. Chen, Y. Zhang, H. Lu, J. Ding, X. Wang, Y. Huang, H. Ma, J. Wang, *eScience* **2023**, *3*, 100135.

[37] W. Xue, D. Yu, L. Suo, C. Wang, Z. Wang, G. Xu, X. Xiao, M. Ge, M. Ko, Y. Chen, L. Qie, Z. Zhu, A. S. Helal, W.-K. Lee, J. Li, *Matter* **2019**, *1*, 1047.

[38] W. Xue, Q.-B. Yan, G. Xu, L. Suo, Y. Chen, C. Wang, C.-A. Wang, J. Li, *Nano Energy* **2017**, *38*, 12.

[39] K. Xu, *J. Electrochem. Soc.* **2009**, *156*, A751.

[40] J. Qian, W. A. Henderson, W. Xu, P. Bhattacharya, M. Engelhard, O. Borodin, J.-G. Zhang, *Nat. Commun.* **2015**, *6*, 6362.

[41] P. Bai, J. Li, F. R. Brushett, M. Z. Bazant, *Energy Environ. Sci.* **2016**, *9*, 3221.

[42] J. Steiger, D. Kramer, R. Mönig, *Electrochim. Acta* **2014**, *136*, 529.

[43] W. Cao, Q. Li, X. Yu, H. Li, *eScience* **2022**, *2*, 47.

[44] H. J. S. Sand, *Philos. Mag.* **2010**, *1*, 45.

[45] J.-F. Ding, Y.-T. Zhang, R. Xu, R. Zhang, Y. Xiao, S. Zhang, C.-X. Bi, C. Tang, R. Xiang, H. S. Park, Q. Zhang, J.-Q. Huang, *Green Energy Environ.* **2023**, *8*, 1509.

[46] H. Ghassemi, M. Au, N. Chen, P. A. Heiden, R. S. Yassar, *Appl. Phys. Lett.* **2011**, *99*, 123113.

[47] R. L. Sacci, N. J. Dudney, K. L. More, L. R. Parent, I. Arslan, N. D. Browning, R. R. Unocic, *Chem. Commun.* **2014**, *50*, 2104.

[48] J. B. Goodenough, Y. Kim, *Chem. Mater.* **2009**, *22*, 587.

[49] A. Ramasubramanian, V. Yurkiv, T. Foroozan, M. Ragone, R. Shahbazian-Yassar, F. Mashayek, *J. Phys.Chem. C* **2019**, *123*, 10237.

[50] E. Peled, D. Golodnitsky, G. Ardel, *J. Electrochem. Soc.* **1997**, *144*, L208.

[51] Y. Li, Y. Li, A. Pei, K. Yan, Y. Sun, C.-L. Wu, L.-M. Joubert, R. Chin, A. L. Koh, Y. Yu, J. Perrino, B. Butz, S. Chu, Y. Cui, *Science* **2017**, *258*, 506.

[52] Y. Li, W. Huang, Y. Li, A. Pei, D. T. Boyle, Y. Cui, *Joule* **2018**, *2*, 2167.

[53] Y. Zhou, M. Su, X. Yu, Y. Zhang, J.-G. Wang, X. Ren, R. Cao, W. Xu, D. R. Baer, Y. Du, O. Borodin, Y. Wang, X.-L. Wang, K. Xu, Z. Xu, C. Wang, Z. Zhu, *Nat. Nanotechnol.* **2020**, *15*, 224.

[54] Y. Jin, N.-J. H. Kneusels, P. C. M. M. Magusin, G. Kim, E. Castillo-Martinez, L. E. Marbella, R. N. Kerber, D. J. Howe, S. Paul, T. Liu, C. P. Grey, *J. Am. Chem. Soc.* **2017**, *139*, 14992.

[55] D. Aurbach, M. L. Daroux, P. W. Faguy, E. Yeager, *J. Electrochem. Soc.* **1987**, *134*, 1611.

[56] L. Suo, W. Xue, M. Gobet, S. G. Greenbaum, C. Wang, Y. Chen, W. Yang, Y. Li, J. Li, *Proc. Natl. Acad. Sci. USA* **2018**, *115*, 1156.

[57] W. Cai, Y. Deng, Z. Deng, Y. Jia, Z. Li, X. Zhang, C. Xu, X. Q. Zhang, Y. Zhang, Q. Zhang, *Adv. Energy Mater.* **2023**, *13*, 2301396.

[58] C. Luo, Q. Liu, X. Wang, Y. Tian, Z. Liu, F. Kang, B. Li, *Nano Energy* **2023**, *109*, 108323.

[59] C.-C. Su, M. He, M. Cai, J. Shi, R. Amine, N. D. Rago, J. Guo, T. Rojas, A. T. Ngo, K. Amine, *Nano Energy* **2022**, *92*, 106720.

[60] Z. Deng, Y. Jia, Y. Deng, C. Xu, X. Zhang, Q. He, J. Peng, H. Wu, W. Cai, *J. Energy Chem.* **2024**, *96*, 282.

[61] X. Fan, X. Ji, L. Chen, J. Chen, T. Deng, F. Han, J. Yue, N. Piao, R. Wang, X. Zhou, X. Xiao, L. Chen, C. Wang, *Nat. Energy* **2019**, *4*, 882.

[62] Z. Li, Y. Chen, X. Yun, P. Gao, C. Zheng, P. Xiao, *Adv. Funct. Mater.* **2023**, *33*, 2300502.

[63] H. Wang, Z. Yu, X. Kong, S. C. Kim, D. T. Boyle, J. Qin, Z. Bao, Y. Cui, *Joule* **2022**, *6*, 588.

[64] J. Wang, Q. Zheng, M. Fang, S. Ko, Y. Yamada, A. Yamada, *Adv. Sci.* **2021**, *8*, 2101646.

[65] X. Cao, P. Gao, X. Ren, L. Zou, M. H. Engelhard, B. E. Matthews, J. Hu, C. Niu, D. Liu, B. W. Arey, C. Wang, J. Xiao, J. Liu, W. Xu, J.-G. Zhang, *Proc. Natl. Acad. Sci. USA* **2021**, *118*, 2020357118.

[66] X. Ren, S. Chen, H. Lee, D. Mei, M. H. Engelhard, S. D. Burton, W. Zhao, J. Zheng, Q. Li, M. S. Ding, M. Schroeder, J. Alvarado, K. Xu, Y. S. Meng, J. Liu, J.-G. Zhang, W. Xu, *Chem* **2018**, *4*, 1877.

[67] J. Wang, Y. Yamada, K. Sodeyama, E. Watanabe, K. Takada, Y. Tateyama, A. Yamada, *Nat. Energy* **2017**, *3*, 22.

[68] X. Ren, P. Gao, L. Zou, S. Jiao, X. Cao, X. Zhang, H. Jia, M. H. Engelhard, B. E. Matthews, H. Wu, H. Lee, C. Niu, C. Wang, B. W. Arey, J. Xiao, J. Liu, J.-G. Zhang, W. Xu, *Proc. Natl. Acad. Sci. USA* **2020**, *117*, 28603.

[69] L. Suo, B. Oleg, T. Gao, K. Xu, *Science* **2015**, *350*, 938.

[70] C. Tian, K. Qin, L. Suo, *Mater. Futhures* **2023**, *2*, 012101.

[71] X. Fan, L. Chen, X. Ji, T. Deng, S. Hou, J. Chen, J. Zheng, F. Wang, J. Jiang, K. Xu, C. Wang, *Chem* **2018**, *4*, 174.

[72] L. Lin, K. Qin, Q. Zhang, L. Gu, L. Suo, Y.s. Hu, H. Li, X. Huang, L. Chen, *Angew. Chem., Int. Ed.* **2021**, *60*, 8289.

[73] J. Wang, Y. Yamada, K. Sodeyama, C. H. Chiang, Y. Tateyama, A. Yamada, *Nat. Commun.* **2016**, *7*, 12032.

[74] L. Dong, Y. Liu, D. Chen, Y. Han, Y. Ji, J. Liu, B. Yuan, Y. Dong, Q. Li, S. Zhou, S. Zhong, Y. Liang, M. Yang, C. Yang, W. He, *Energy Storage Mater.* **2022**, *44*, 527.

[75] L. Suo, Y.-S. Hu, H. Li, M. Armand, L. Chen, *Nat. Commun.* **2013**, *4*, 1481.

[76] S. Chen, Y. Xiang, G. Zheng, Y. Liao, F. Ren, Y. Zheng, H. He, B. Zheng, X. Liu, N. Xu, M. Luo, J. Zheng, Y. Yang, *ACS Appl. Mater. Interfaces* **2020**, *12*, 27794.

[77] X. Cao, H. Jia, W. Xu, J.-G. Zhang, *J. Electrochem. Soc.* **2021**, *168*, 010522.

[78] Y. Yamada, A. Yamada, *J. Electrochem. Soc.* **2015**, *162*, A2406.

[79] Y. Jie, X. Ren, R. Cao, W. Cai, S. Jiao, *Adv. Funct. Mater.* **2020**, *30*, 1910777.

[80] T. T. Hagos, B. Thirumalraj, C.-J. Huang, L. H. Abrha, T. M. Hagos, G. B. Berhe, H. K. Bezabh, J. Cherng, S.-F. Chiu, W.-N. Su, B.-J. Hwang, *ACS Appl. Mater. Interfaces* **2019**, *11*, 9955.

[81] X. Ren, L. Zou, X. Cao, M. H. Engelhard, W. Liu, S. D. Burton, H. Lee, C. Niu, B. E. Matthews, Z. Zhu, C. Wang, B. W. Arey, J. Xiao, J. Liu, J.-G. Zhang, W. Xu, *Joule* **2019**, *3*, 1662.

[82] N. Ehteshami, L. Ibing, L. Stolz, M. Winter, E. Paillard, *J. Power Sources* **2020**, *451*, 227804.

[83] E. Markevich, G. Salitra, D. Aurbach, *ACS Energy Lett.* **2017**, *2*, 1337.

[84] E. Markevich, G. Salitra, F. Chesneau, M. Schmidt, D. Aurbach, *ACS Energy Lett.* **2017**, *2*, 1321.

[85] C.-C. Su, M. He, R. Amine, Z. Chen, R. Sahore, N. Dietz Rago, K. Amine, *Energy Storage Mater.* **2019**, *17*, 284.

[86] Y. Yang, W. H. Yang, H. J. Yang, H. S. Zhou, *eScience* **2023**, *3*, 100170.

[87] Z. Wang, Z. Sun, Y. Shi, F. Qi, X. Gao, H. Yang, H. M. Cheng, F. Li, *Adv. Energy Mater.* **2021**, *11*, 2100935.

[88] M. Mao, X. Ji, Q. Wang, Z. Lin, M. Li, T. Liu, C. Wang, Y.-S. Hu, H. Li, X. Huang, L. Chen, L. Suo, *Nat. Commun.* **2023**, *14*, 1082.

[89] X. Fan, L. Chen, O. Borodin, X. Ji, J. Chen, S. Hou, T. Deng, J. Zheng, C. Yang, S.-C. Liou, K. Amine, K. Xu, C. Wang, *Nat. Nanotechnol.* **2018**, *13*, 715.

[90] P. Xiao, Y. Zhao, Z. Piao, B. Li, G. Zhou, H.-M. Cheng, *Energy Environ. Sci.* **2022**, *15*, 2435.

[91] Q. Wang, Z. Yao, C. Zhao, T. Verhallen, D. P. Tabor, M. Liu, F. Ooms, F. Kang, A. Aspuru-Guzik, Y.-S. Hu, M. Wagemaker, B. Li, *Nat. Commun.* **2020**, *11*, 4188.

[92] S. Weng, X. Zhang, G. Yang, S. Zhang, B. Ma, Q. Liu, Y. Liu, C. Peng, H. Chen, H. Yu, X. Fan, T. Cheng, L. Chen, Y. Li, Z. Wang, X. Wang, *Nat. Commun.* **2023**, *14*, 4474.

[93] J. Holoubek, M. Yu, S. Yu, M. Li, Z. Wu, D. Xia, P. Bhaladhare, M. S. Gonzalez, T. A. Pascal, P. Liu, Z. Chen, *ACS Energy Lett.* **2020**, *5*, 1438.

[94] S. Yang, M. Hao, Z. Wang, Z. Xie, Z. Cai, M. Hu, B. Chen, L. Wang, K. Zhou, *Chem. Eng. J.* **2022**, *435*, 134897.

[95] J. Wu, Z. Gao, Y. Tian, Y. Zhao, Y. Lin, K. Wang, H. Guo, Y. Pan, X. Wang, F. Kang, N. Tavajohi, X. Fan, B. Li, *Adv. Mater.* **2023**, *35*, 2303347.

[96] K. Ding, C. Xu, Z. Peng, X. Long, J. Shi, Z. Li, Y. Zhang, J. Lai, L. Chen, Y.-P. Cai, Q. Zheng, *ACS Appl. Mater. Interfaces* **2022**, *14*, 44470.

[97] Z. Wang, C. Chen, D. Wang, Y. Zhu, B. Zhang, *Angew. Chem., Int. Ed.* **2023**, *62*, 202303950.

[98] J. Zhang, Q. Li, Y. Zeng, Z. Tang, D. Sun, D. Huang, Y. Tang, H. Wang, *ACS Energy Lett.* **2023**, *8*, 1752.

[99] T. Ma, Y. Ni, Q. Wang, W. Zhang, S. Jin, S. Zheng, X. Yang, Y. Hou, Z. Tao, J. Chen, *Angew. Chem., Int. Ed.* **2022**, *61*, 202207927.

[100] Y. Chen, Z. Yu, P. Rudnicki, H. Gong, Z. Huang, S. C. Kim, J.-C. Lai, X. Kong, J. Qin, Y. Cui, Z. Bao, *J. Am. Chem. Soc.* **2021**, *143*, 18703.

[101] T. D. Pham, K. K. Lee, *Small* **2021**, *17*, 2100133.

[102] J. Holoubek, H. Liu, Z. Wu, Y. Yin, X. Xing, G. Cai, S. Yu, H. Zhou, T. A. Pascal, Z. Chen, P. Liu, *Nat. Energy* **2021**, *6*, 303.

[103] A.-M. Li, O. Borodin, T. P. Pollard, W. Zhang, N. Zhang, S. Tan, F. Chen, C. Jayawardana, B. L. Lucht, E. Hu, X.-Q. Yang, C. Wang, *Nat. Chem.* **2024**, 922.

[104] S. Chen, J. Fan, Z. Cui, L. Tan, D. Ruan, X. Zhao, J. Jiang, S. Jiao, X. Ren, *Angew. Chem., Int. Ed.* **2023**, *62*, 202219310.

[105] A. Dutta, K. Matsushita, Y. Kubo, *Adv. Sci.* **2024**, 2404245.

[106] V. Marangon, C. Hernandez-Rentero, S. Levchenko, G. Bianchini, D. Spagnolo, A. Caballero, J. Morales, J. Hassoun, *ACS Appl. Energy Mater.* **2020**, *3*, 12263.

[107] J.-J. Xu, Z.-L. Wang, D. Xu, F.-Z. Meng, X.-B. Zhang, *Energy Environ. Sci.* **2014**, *7*, 2213.

[108] R. Black, J.-H. Lee, B. Adams, C. A. Mims, L. F. Nazar, *Angew. Chem., Int. Ed.* **2013**, *52*, 392.

[109] S. Chen, W. Zhu, L. Tan, D. Ruan, J. Fan, Y. Chen, X. Meng, Q. Nian, X. Zhao, J. Jiang, Z. Wang, S. Jiao, X. Wu, X. Ren, *ACS Appl. Mater. Interfaces* **2023**, *15*, 13155.

[110] Y. Zhao, T. Zhou, L. P. H. Jeurgens, X. Kong, J. W. Choi, A. Coskun, *Chem* **2023**, *9*, 682.

[111] R. Wang, J. Li, B. Han, Q. Wang, R. Ke, T. Zhang, X. Ao, G. Zhang, Z. Liu, Y. Qian, F. Pan, I. Lynch, J. Wang, Y. Deng, *J. Energy Chem.* **2023**, *88*, 532.

[112] Z. Yu, H. Wang, X. Kong, W. Huang, Y. Tsao, D. G. Mackanic, K. Wang, X. Wang, W. Huang, S. Choudhury, Y. Zheng, C. V. Amanchukwu, S. T. Hung, Y. Ma, E. G. Lomeli, J. Qin, Y. Cui, Z. Bao, *Nat. Energy* **2020**, *5*, 526.

[113] Z. Yu, P. E. Rudnicki, Z. Zhang, Z. Huang, H. Celik, S. T. Oyakhire, Y. Chen, X. Kong, S. C. Kim, X. Xiao, H. Wang, Y. Zheng, G. A. Kamat, M. S. Kim, S. F. Bent, J. Qin, Y. Cui, Z. Bao, *Nat. Energy* **2022**, *7*, 94.

[114] L.-Q. Wu, Z. Li, Z.-Y. Fan, K. Li, J. Li, D. Huang, A. Li, Y. Yang, W. Xie, Q. Zhao, *J. Am. Chem. Soc.* **2024**, *146*, 5964.

[115] D. Ruan, L. Tan, S. Chen, J. Fan, Q. Nian, L. Chen, Z. Wang, X. Ren, *JACS Au* **2023**, *3*, 953.

[116] G. Zhang, X. Deng, J. Li, J. Wang, G. Shi, Y. Yang, J. Chang, K. Yu, S.-S. Chi, H. Wang, P. Wang, Z. Liu, Y. Gao, Z. Zheng, Y. Deng, C. Wang, *Nano Energy* **2022**, *95*, 107014.

[117] J. Zhang, H. Zhang, R. Li, L. Lv, D. Lu, S. Zhang, X. Xiao, S. Geng, F. Wang, T. Deng, L. Chen, X. Fan, *J. Energy Chem.* **2023**, *78*, 71.

[118] Y. Zhao, T. Zhou, M. Mensi, J. W. Choi, A. Coskun, *Nat. Commun.* **2023**, *14*, 299.

[119] J. Chen, H. Lu, X. Kong, J. Liu, J. Liu, J. Yang, Y. Nuli, J. Wang, *Angew. Chem., Int. Ed.* **2024**, *63*, 202317923.

[120] F. Liu, W. Wang, Y. Yin, S. Zhang, J. Shi, L. Wang, X. Zhang, Y. Zheng, J. Zhou, L. Li, Y. Guo, *Sci. Adv.* **2018**, *4*, eaat5383.

[121] X. Peng, T. Wang, B. Liu, Y. Li, T. Zhao, *Energy Environ. Sci.* **2022**, *15*, 5350.

[122] Y. Zhao, T. Zhou, T. Ashirov, M. E. Kazzi, C. Cancellieri, L. P. H. Jeurgens, J. W. Choi, A. Coskun, *Nat. Commun.* **2022**, *13*, 2575.

[123] T. Zhou, Y. Zhao, M. El Kazzi, J. W. Choi, A. Coskun, *Angew. Chem., Int. Ed.* **2022**, *61*, 202115884.

[124] Y. Zhao, T. Zhou, D. Baster, M. El Kazzi, J. W. Choi, A. Coskun, *ACS Energy Lett.* **2023**, *8*, 3180.

[125] Y. Zhao, T. Zhou, M. El Kazzi, A. Coskun, *ACS Appl. Energy Mater.* **2022**, *5*, 7784.

[126] K. Lee, S.-H. Kwon, J. Kim, E. Park, I. Kim, H. C. Ahn, A. Coskun, J. W. Choi, *ACS Energy Lett.* **2024**, 2201.

[127] G.-X. Li, V. Koverga, A. Nguyen, R. Kou, M. Ncube, H. Jiang, K. Wang, M. Liao, H. Guo, J. Chen, N. Dandu, A. T. Ngo, D. Wang, *Nat. Energy* **2024**, *9*, 817.

[128] H. Moon, T. Mandai, R. Tatara, K. Ueno, A. Yamazaki, K. Yoshida, S. Seki, K. Dokko, M. Watanabe, *J. Phys. Chem. C* **2015**, *119*, 3957.

[129] S. Chen, J. Zheng, D. Mei, K. S. Han, M. H. Engelhard, W. Zhao, W. Xu, J. Liu, J.-G. Zhang, *Adv. Mater.* **2018**, *30*, 1706102.

[130] K. Park, Y. Jo, B. Koo, H. Lee, H. Lee, *Chem. Eng. J.* **2022**, *427*, 131889.

[131] A. L. Li, G.-H. Li, S.-G. Lu, Z.-M. Ren, J.-T. Wang, H.-X. Zhuo, W. Quan, G.-N. Zhang, F.-J. Han, Y.-M. Xia, J. Wang, Y. Zhang, *Rare Met.* **2021**, *41*, 822.

[132] X. Cao, L. Zou, B. E. Matthews, L. Zhang, X. He, X. Ren, M. H. Engelhard, S. D. Burton, P. Z. El-Khoury, H.-S. Lim, C. Niu, H. Lee, C. Wang, B. W. Arey, C. Wang, J. Xiao, J. Liu, W. Xu, J.-G. Zhang, *Energy Storage Mater.* **2021**, *34*, 76.

[133] Y. Zheng, F. A. Soto, V. Ponce, J. M. Seminario, X. Cao, J.-G. Zhang, P. B. Balbuena, *J. Mater. Chem. A* **2019**, *7*, 25047.

[134] T. Doi, Y. Shimizu, M. Hashinokuchi, M. Inaba, *J. Electrochem. Soc.* **2017**, *164*, A6412.

[135] J. Zheng, G. Ji, X. Fan, J. Chen, Q. Li, H. Wang, Y. Yang, K. C. DeMella, S. R. Raghavan, C. Wang, *Adv. Energy Mater.* **2019**, *9*, 1614.

[136] Z. Cui, Z. Jia, D. Ruan, Q. Nian, J. Fan, S. Chen, Z. He, D. Wang, J. Jiang, J. Ma, X. Ou, S. Jiao, Q. Wang, X. Ren, *Nat. Commun.* **2024**, *15*, 2033.

[137] W. Xue, Z. Shi, M. Huang, S. Feng, C. Wang, F. Wang, J. Lopez, B. Qiao, G. Xu, W. Zhang, Y. Dong, R. Gao, Y. Shao-Horn, J. A. Johnson, J. Li, *Energy Environ. Sci.* **2020**, *13*, 212.

[138] W. Xue, M. Huang, Y. Li, Y. G. Zhu, R. Gao, X. Xiao, W. Zhang, S. Li, G. Xu, Y. Yu, P. Li, J. Lopez, D. Yu, Y. Dong, W. Fan, Z. Shi, R. Xiong, C.-J. Sun, I. Hwang, W.-K. Lee, Y. Shao-Horn, J. A. Johnson, J. Li, *Nat. Energy* **2021**, *6*, 495.

[139] W. Xue, R. Gao, Z. Shi, X. Xiao, W. Zhang, Y. Zhang, Y. G. Zhu, I. Waluyo, Y. Li, M. R. Hill, Z. Zhu, S. Li, O. Kuznetsov, Y. Zhang, W.-K. Lee, A. Hunt, A. Harutyunyan, Y. Shao-Horn, J. A. Johnson, J. Li, *Energy Environ. Sci.* **2021**, *14*, 6030.

[140] G. Zhang, J. Li, Q. Wang, H. Wang, J. Wang, K. Yu, J. Chang, C. Wang, X. Hong, Q. Ma, Y. Deng, *ACS Energy Lett.* **2023**, *8*, 2868.

[141] S. Kim, J. H. Jeon, K. Park, S. H. Kweon, J. H. Hyun, C. Song, D. Lee, G. Song, S. H. Yu, T. K. Lee, S. K. Kwak, K. T. Lee, S. Y. Hong, N. S. Choi, *Adv. Mater.* **2024**, *36*, 2401615.

[142] C. Sun, R. Li, S. Weng, C. Zhu, L. Chen, S. Jiang, L. Li, X. Xiao, C. Liu, L. Chen, T. Deng, X. Wang, X. Fan, *Angew. Chem., Int. Ed.* **2024**, *63*, 202400761.

[143] T. Liu, Z. Shi, H. Li, W. Xue, S. Liu, J. Yue, M. Mao, Y.s. Hu, H. Li, X. Huang, L. Chen, L. Suo, *Adv. Mater.* **2021**, *33*, 2102034.

[144] Y. Huang, R. Li, S. Weng, H. Zhang, C. Zhu, D. Lu, C. Sun, X. Huang, T. Deng, L. Fan, L. Chen, X. Wang, X. Fan, *Energy Environ. Sci.* **2022**, *15*, 4349.

[145] C. Sun, R. Li, C. Zhu, L. Chen, S. Weng, C. Liu, T. Deng, L. Chen, X. Wang, X. Fan, *ACS Energy Lett.* **2023**, *8*, 4119.

[146] G. M. Hobold, C. Wang, K. Steinberg, Y. Li, B. M. Gallant, *Nat. Energy* **2024**, *9*, 580.

[147] R. Guo, B. M. Gallant, *Chem. Mater.* **2020**, *32*, 5525.

[148] R. May, K. J. Fritzsching, D. Livitz, S. R. Denny, L. E. Marbella, *ACS Energy Lett.* **2021**, 1162.

[149] M. S. Kim, Z. Zhang, P. E. Rudnicki, Z. Yu, J. Wang, H. Wang, S. T. Oyakhire, Y. Chen, S. C. Kim, W. Zhang, D. T. Boyle, X. Kong, R. Xu, Z. Huang, W. Huang, S. F. Bent, L. W. Wang, J. Qin, Z. Bao, Y. Cui, *Nat. Mater.* **2022**, *21*, 445.

[150] M. S. Kim, Z. Zhang, J. Wang, S. T. Oyakhire, S. C. Kim, Z. Yu, Y. Chen, D. T. Boyle, Y. Ye, Z. Huang, W. Zhang, R. Xu, P. Sayavong, S. F. Bent, J. Qin, Z. Bao, Y. Cui, *ACS Nano* **2023**, *17*, 3168.

[151] X. Zhang, P. Xu, J. Duan, X. Lin, J. Sun, W. Shi, H. Xu, W. Dou, Q. Zheng, R. Yuan, J. Wang, Y. Zhang, S. Yu, Z. Chen, M. Zheng, J.-F. Gohy, Q. Dong, A. Vlad, *Nat. Commun.* **2024**, *15*, 536.

[152] T. Taskovic, A. Eldesoky, C. P. Aiken, J. R. Dahn, *J. Electrochem. Soc.* **2022**, *169*, 100547.

[153] F. Hai, Y. Yi, Z. Xiao, J. Guo, X. Gao, W. Chen, W. Xue, W. Hua, W. Tang, M. Li, *Adv. Energy Mater.* **2024**, *14*, 2304253.

[154] C. V. Amanchukwu, X. Kong, J. Qin, Y. Cui, Z. Bao, *Adv. Energy Mater.* **2019**, *9*, 1902116.

[155] T. Liu, H. Li, J. Yue, J. Feng, M. Mao, X. Zhu, Y.s. Hu, H. Li, X. Huang, L. Chen, L. Suo, *Angew. Chem., Int. Ed.* **2021**, *60*, 17547.

[156] M. L. Mao, L. Gong, X. B. Wang, Q. Y. Wang, G. Q. Zhang, H. X. Wang, W. Xie, L. M. Suo, C. L. Wang, *Proc. Natl. Acad. Sci. USA* **2024**, *121*, 2316212121.

[157] L. Tan, S. Chen, Y. Chen, J. Fan, D. Ruan, Q. Nian, L. Chen, S. Jiao, X. Ren, *Angew. Chem., Int. Ed.* **2022**, *61*, 202203693.

[158] C. S. Rustomji, Y. Yang, T. K. Kim, J. Mac, Y. J. Kim, E. Caldwell, H. Chung, Y. S. Meng, *Science* **2017**, *356*, eaal4263.

[159] Y. Yang, D. M. Davies, Y. Yin, O. Borodin, J. Z. Lee, C. Fang, M. Olguin, Y. Zhang, E. S. Sablina, X. Wang, C. S. Rustomji, Y. S. Meng, *Joule* **2019**, *3*, 1986.

[160] Y. Yang, Y. Yin, D. M. Davies, M. Zhang, M. Mayer, Y. Zhang, E. S. Sablina, S. Wang, J. Z. Lee, O. Borodin, C. S. Rustomji, Y. S. Meng, *Energy Environ. Sci.* **2020**, *13*, 2209.

[161] Y. Yin, Y. Yang, D. Cheng, M. Mayer, J. Holoubek, W. Li, G. Raghavendran, A. Liu, B. Lu, D. M. Davies, Z. Chen, O. Borodin, Y. S. Meng, *Nat. Energy* **2022**, *7*, 548.

[162] Z. Wu, R. Li, S. Zhang, L. lv, T. Deng, H. Zhang, R. Zhang, J. Liu, S. Ding, L. Fan, L. Chen, X. Fan, *Chem* **2023**, *9*, 650.

[163] Z. Xu, K. Deng, S. Zhou, D. Mo, *J. Power Sources* **2023**, *559*, 232631.

[164] R. Li, Z. Wu, S. Zhang, J. Liu, L. Fan, T. Deng, L. Chen, X. Fan, *Angew. Chem., Int. Ed.* **2024**, 202406122.

[165] T. Ma, G.-L. Xu, Y. Li, L. Wang, X. He, J. Zheng, J. Liu, M. H. Engelhard, P. Zapol, L. A. Curtiss, J. Jorne, K. Arnine, Z. Chen, *J. Phys. Chem. Lett.* **2017**, *8*, 1072.

[166] M. Morita, T. Shibata, N. Yoshimoto, M. Ishikawa, *Electrochim. Acta* **2002**, *47*, 2787.

[167] H. Yang, K. Kwon, T. M. Devine, J. W. Evans, *J. Electrochem. Soc.* **2000**, *147*, 4399.

[168] L. Qiao, U. Oteo, M. Martinez-Ibañez, A. Santiago, R. Cid, E. Sanchez-Diez, E. Lobato, L. Meabe, M. Armand, H. Zhang, *Nat. Mater.* **2022**, *21*, 455.

[169] L. Li, G. Xu, S. Zhang, S. Dong, S. Wang, Z. Cui, X. Du, C. Wang, B. Xie, J. Du, X. Zhou, G. Cui, *ACS Energy Lett.* **2022**, *7*, 591.

[170] Y. Xia, P. Zhou, X. Kong, J. Tian, W. Zhang, S. Yan, W.-h. Hou, H.-Y. Zhou, H. Dong, X. Chen, P. Wang, Z. Xu, L. Wan, B. Wang, K. Liu, *Nat. Energy* **2023**, *8*, 934.

[171] P. Zhou, H. Zhou, Y. Xia, Q. Feng, X. Kong, W. Hou, Y. Ou, X. Song, H.-y. Zhou, W. Zhang, Y. Lu, F. Liu, Q. Cao, H. Liu, S. Yan, K. Liu, *Angew. Chem., Int. Ed.* **2024**, *136*, 202316717.

[172] Z. Piao, H. R. Ren, G. Lu, K. Jia, J. Tan, X. Wu, Z. Zhuang, Z. Han, C. Li, R. Gao, X. Tao, G. Zhou, H. M. Cheng, *Angew. Chem., Int. Ed.* **2023**, *62*, 202300966.

[173] S. Jiao, X. Ren, R. Cao, M. H. Engelhard, Y. Liu, D. Hu, D. Mei, J. Zheng, W. Zhao, Q. Li, N. Liu, B. D. Adams, C. Ma, J. Liu, J.-G. Zhang, W. Xu, *Nat. Energy* **2018**, *3*, 739.

[174] R. Weber, M. Genovese, A. J. Louli, S. Hames, C. Martin, I. G. Hill, J. R. Dahn, *Nat. Energy* **2019**, *4*, 683.

[175] M. Genovese, A. J. Louli, R. Weber, S. Hames, J. R. Dahn, *J. Electrochem. Soc.* **2018**, *165*, A3321.

[176] A. J. Louli, M. Coon, M. Genovese, J. deGooyer, A. Eldesoky, J. R. Dahn, *J. Electrochem. Soc.* **2021**, *168*, 020515.

[177] N. Li, Y. Tong, H. Li, L. Wang, F. Hou, S. X. Dou, J. Liang, *Carbon* **2021**, *182*, 233.

[178] Y. M. Lee, J. E. Seo, N.-S. Choi, J.-K. Park, *Electrochim. Acta* **2005**, *50*, 2843.

[179] M. Herstedt, M. Stjerndahl, T. Gustafsson, K. Edström, *Electrochem. Commun.* **2003**, *5*, 467.

[180] K. Huang, S. Bi, B. Kurt, C. Xu, L. Wu, Z. Li, G. Feng, X. Zhang, *Angew. Chem., Int. Ed.* **2021**, *60*, 19232.
[181] J. Liu, X. Li, J. Huang, G. Yang, J. Ma, *Adv. Funct. Mater.* **2024**, *34*, 2212762.
[182] Q. Liu, G. Yang, S. Li, S. Zhang, R. Chen, Z. Wang, L. Chen, *ACS Appl. Mater. Interfaces* **2021**, *13*, 21459.
[183] W. Gu, G. Xue, Q. Dong, R. Yi, Y. Mao, L. Zheng, H. Zhang, X. Fan, Y. Shen, L. Chen, *eScience* **2022**, *2*, 486.
[184] Y. Li, K. Wang, J. Chen, W. Zhang, X. Luo, Z. Hu, Q. Zhang, L. Xing, W. Li, *ACS Appl. Mater. Interfaces* **2020**, *12*, 28169.
[185] Y. Wang, Z. Wang, L. Zhao, Q. Fan, X. Zeng, S. Liu, W. K. Pang, Y. B. He, Z. Guo, *Adv. Mater.* **2021**, *33*, 2008133.
[186] T. Inose, S. Tada, H. Morimoto, S.-i. Tobishima, *J. Power Sources* **2006**, *161*, 550.
[187] H. Chen, J. Chen, W. Zhang, Q. Xie, Y. Che, H. Wang, L. Xing, K. Xu, W. Li, *J. Mater. Chem. A* **2020**, *8*, 22054.
[188] B. Tong, J. Wang, Z. Liu, L. Ma, P. Wang, W. Feng, Z. Peng, Z. Zhou, *J. Power Sources* **2018**, *400*, 225.
[189] S. S. Zhang, *Electrochim. Acta* **2012**, *70*, 344.
[190] V. Y. Mikhaylik, Tucson, AZ, US. 20080187840, **2008**.
[191] F. Qiu, X. Li, H. Deng, D. Wang, X. Mu, P. He, H. Zhou, *Adv. Energy Mater.* **2018**, *9*, 1803372.
[192] X. Li, R. X. Zhao, Y. Z. Fu, A. Manthiram, *eScience* **2021**, *1*, 108.
[193] S. Kim, S. O. Park, M.-Y. Lee, J.-A. Lee, I. Kristanto, T. K. Lee, D. Hwang, J. Kim, T.-U. Wi, H.-W. Lee, S. K. Kwak, N.-S. Choi, *Energy Storage Mater.* **2022**, *45*, 1.
[194] X. Wang, S. Li, W. Zhang, D. Wang, Z. Shen, J. Zheng, H. L. Zhuang, Y. He, Y. Lu, *Nano Energy* **2021**, *89*, 106353.
[195] P. Zhou, Y. Xia, Y. Wu, W.-h. Hou, Y. Lu, S. S. Yan, H.-y. Zhou, W. Zhang, K. Liu, *ACS Appl. Mater. Interfaces* **2022**, *14*, 38921.
[196] X.-Q. Zhang, X. Chen, L.-P. Hou, B.-Q. Li, X.-B. Cheng, J.-Q. Huang, Q. Zhang, *ACS Energy Lett.* **2019**, *4*, 411.
[197] D. Aurbach, E. Pollak, R. Elazari, G. Salitra, C. S. Kelley, J. Affinito, *J. Electrochem. Soc.* **2009**, *156*, A694.
[198] S. Xiong, K. Xie, Y. Diao, X. Hong, *Electrochim. Acta* **2012**, *83*, 78.
[199] W. Li, H. Yao, K. Yan, G. Zheng, Z. Liang, Y.-M. Chiang, Y. Cui, *Nat. Commun.* **2015**, *6*, 7436.
[200] C. Yan, Y. X. Yao, X. Chen, X. B. Cheng, X. Q. Zhang, J. Q. Huang, Q. Zhang, *Angew. Chem., Int. Ed.* **2018**, *57*, 14055.
[201] M. M. Rahman, S. Tan, Y. Yang, H. Zhong, S. Ghose, I. Waluyo, A. Hunt, L. Ma, X.-Q. Yang, E. Hu, *Nat. Commun.* **2023**, *14*, 8414.
[202] S. Gu, S. W. Zhang, J. Han, Y. Deng, C. Luo, G. Zhou, Y. He, G. Wei, F. Kang, W. Lv, Q. H. Yang, *Adv. Funct. Mater.* **2021**, *31*, 2102128.
[203] F. Ding, W. Xu, G. L. Graff, J. Zhang, M. L. Sushko, X. Chen, Y. Shao, M. H. Engelhard, Z. Nie, J. Xiao, X. Liu, P. V. Sushko, J. Liu, J.-G. Zhang, *J. Am. Chem. Soc.* **2013**, *135*, 4450.
[204] Z. Xie, Z. Wu, X. An, X. Yue, A. Yoshida, X. Du, X. Hao, A. Abudula, G. Guan, *Chem. Eng. J.* **2020**, *393*, 124789.
[205] T. Zhang, Y. Li, N. Chen, Z. Wen, Y. Shang, Y. Zhao, M. Yan, M. Guan, F. Wu, R. Chen, *ACS Appl. Mater. Interfaces* **2021**, *13*, 681.
[206] S. Zhang, S. Li, Y. Lu, *eScience* **2021**, *1*, 163.
[207] Q. Liu, Z. Chen, Y. Liu, Y. Hong, W. Wang, J. Wang, B. Zhao, Y. Xu, J. Wang, X. Fan, L. Li, H. B. Wu, *Energy Storage Mater.* **2021**, *37*, 521.
[208] Y. Lu, W. Zhang, S. Liu, Q. Cao, S. Yan, H. Liu, W. Hou, P. Zhou, X. Song, Y. Ou, Y. Li, K. Liu, *ACS Nano* **2023**, *17*, 9586.
[209] Q. Liu, Y. Liu, Z. Chen, Q. Ma, Y. Hong, J. Wang, Y. Xu, W. Zhao, Z. Hu, X. Hong, J. Wang, X. Fan, H. B. Wu, *Adv. Funct. Mater.* **2022**, *33*, 2209725.
[210] C. Miao, S. Qi, K. Liang, Y. Qi, J. Huang, M. Wu, H. Zhao, J. Liu, Y. Ren, J. Ma, *J. Energy Chem.* **2021**, *63*, 566.
[211] X. Li, M. Li, Y. Liu, Y. Jie, W. Li, Y. Chen, F. Huang, Y. Zhang, T. M. Sohail, S. Wang, X. Zhu, T. Cheng, M. D. Gu, S. Jiao, R. Cao, *J. Am. Chem. Soc.* **2024**, *146*, 17023.
[212] D. Feng, S. Chen, R. Wang, T. Chen, S. Gu, J. Su, T. Dong, Y. Liu, *J. Electrochem. Soc.* **2020**, *167*, 110544.
[213] W. Lu, W. Pu, K. Xie, C. Zheng, *ACS Appl. Energy Mater.* **2019**, *3*, 733.
[214] H. Moon, S. Cho, D. Yu, S. Lee, *Energy Environ. Mater.* **2022**, *6*, 2575.
[215] A. Huang, Z. Ma, P. Kumar, H. Liang, T. Cai, F. Zhao, Z. Cao, L. Cavallo, Q. Li, J. Ming, *Nano Lett.* **2024**, *24*, 7499.
[216] K. An, M. J. Joo, Y. H. T. Tran, S. Kwak, H. G. Kim, C. S. Jin, J. Suk, Y. Kang, Y. J. Park, S. W. Song, *Adv. Funct. Mater.* **2023**, *33*, 1616.
[217] N. Piao, X. Gao, H. Yang, Z. Guo, G. Hu, H.-M. Cheng, F. Li, *eTransportation* **2022**, *11*, 100145.
[218] K. Dokko, D. Watanabe, Y. Ugata, M. L. Thomas, S. Tsuzuki, W. Shinoda, K. Hashimoto, K. Ueno, Y. Umebayashi, M. Watanabe, *J. Phys. Chem. B* **2018**, *122*, 10736.
[219] J. Liu, Z. Bao, Y. Cui, E. J. Dufek, J. B. Goodenough, P. Khalifah, Q. Li, B. Y. Liaw, P. Liu, A. Manthiram, Y. S. Meng, V. R. Subramanian, M. F. Toney, V. V. Viswanathan, M. S. Whittingham, J. Xiao, W. Xu, J. Yang, X.-Q. Yang, J.-G. Zhang, *Nat. Energy* **2019**, *4*, 180.
[220] B. D. Adams, J. Zheng, X. Ren, W. Xu, J. Zhang, *Adv. Energy Mater.* **2017**, *8*, 1702097.
[221] Y. Jie, S. Wang, S. Weng, Y. Liu, M. Yang, C. Tang, X. Li, Z. Zhang, Y. Zhang, Y. Chen, F. Huang, Y. Xu, W. Li, Y. Guo, Z. He, X. Ren, Y. Lu, K. Yang, S. Cao, H. Lin, R. Cao, P. Yan, T. Cheng, X. Wang, S. Jiao, D. Xu, *Nat. Energy* **2024**, 2058.
[222] S. Zhang, R. Li, T. Deng, Q. Ma, X. Hong, H. Zhang, R. Zhang, S. Ding, Y. Wu, H. Zhu, M. Li, H. Zhang, D. Lu, B. Ma, L. Lv, Y. Li, L. Chen, Y. Shen, R. Guo, X. Fan, *Nat. Energy* **2024**.
[223] All News-Ses, https://ses.ai/battery-world-us-2023/ (accessed: December, 2023).
[224] C. Niu, H. Lee, S. Chen, Q. Li, J. Du, W. Xu, J.-G. Zhang, M. S. Whittingham, J. Xiao, J. Liu, *Nat. Energy* **2019**, *4*, 551.
[225] Q.-K. Zhang, X.-Q. Zhang, J. Wan, N. Yao, T.-L. Song, J. Xie, L.-P. Hou, M.-Y. Zhou, X. Chen, B.-Q. Li, R. Wen, H.-J. Peng, Q. Zhang, J.-Q. Huang, *Nat. Energy* **2023**, *8*, 725.
[226] Y. Gao, F. Qiao, J. You, Z. Ren, N. Li, K. Zhang, C. Shen, T. Jin, K. Xie, *Nat. Commun.* **2022**, *13*, 2041.
[227] P. Zhao, Y. Li, S. Chen, H. Fan, Y. Feng, L. Hu, Y. Zhang, Q. Nie, H. Pei, C. Yang, J. Deng, C. Bao, J. Song, *Adv. Energy Mater.* **2022**, *12*, 2200568.
[228] W. Deng, W. Dai, X. Zhou, Q. Han, W. Fang, N. Dong, B. He, Z. Liu, *ACS Energy Lett.* **2020**, *6*, 115.
[229] K. Zhang, W. Liu, Y. Gao, X. Wang, Z. Chen, R. Ning, W. Yu, R. Li, L. Li, X. Li, K. Yuan, L. Ma, N. Li, C. Shen, W. Huang, K. Xie, K. P. Loh, *Adv. Mater.* **2020**, *33*, 0935.
[230] L. Zhang, F. Min, Y. Luo, G. Dang, H. Gu, Q. Dong, M. Zhang, L. Sheng, Y. Shen, L. Chen, J. Xie, *Nano Energy* **2022**, *96*, 107122.
[231] L. D. Ellis, J. P. Allen, L. M. Thompson, J. E. Harlow, W. J. Stone, I. G. Hill, J. R. Dahn, *J. Electrochem. Soc.* **2017**, *164*, A3518.
[232] M. Metzger, B. Strehle, S. Solchenbach, H. A. Gasteiger, *J. Electrochem. Soc.* **2016**, *163*, A798.
[233] A. Etxebarria, D. J. Yun, M. Blum, Y. Ye, M. Sun, K. J. Lee, H. Su, M. A. Munoz Marquez, P. N. Ross, E. J. Crumlin, *ACS Appl. Mater.* **2020**, *12*, 26607.
[234] K. N. Shitaw, S. C. Yang, S. K. Jiang, C. J. Huang, N. A. Sahalie, Y. Nikodimos, H. H. Weldeyohannes, C. H. Wang, S. H. Wu, W. N. Su, B. J. Hwang, *Adv. Funct. Mater.* **2020**, *31*, 2006951.
[235] A. J. Louli, M. Genovese, R. Weber, S. G. Hames, E. R. Logan, J. R. Dahn, *J. Electrochem. Soc.* **2019**, *166*, A1291.
[236] A. J. Louli, L. D. Ellis, J. R. Dahn, *Joule* **2019**, *3*, 745.
[237] S. Li, J. Zhang, S. Zhang, Q. Liu, H. Cheng, L. Fan, W. Zhang, X. Wang, Q. Wu, Y. Lu, *Nat. Energy* **2024**, *9*, 285.
[238] A. Rensmo, E. K. Savvidou, I. T. Cousins, X. Hu, S. Schellenberger, J. P. Benskin, *Environ. Sci. Processes Impacts* **2023**, *25*, 1015.

[239] All News-Echa, https://echa.europa.eu/sv/-/echa-publishespfas-restriction-proposal (accessed: February, 2023).
[240] Z. Ren, Z. Ren, Z. Zhang, T. Buonassisi, J. Li, *Nat. Rev. Mater.* **2023**, *8*, 563.
[241] J. Wu, X. Yang, Y. Pan, T. Zuo, Z. Ning, C. Li, Z. Zhang, *J. Flow Chem.* **2023**, *13*, 385.
[242] Y. Chen, Y. He, Y. Gao, J. Xue, W. Qu, J. Xuan, Y. Mo, *Science* **2024**, *384*, 670.
[243] Y. Mo, Z. Lu, G. Rughoobur, P. Patil, N. Gershenfeld, A. I. Akinwande, S. L. Buchwald, K. F. Jensen, *Science* **2020**, *368*, 1352.
[244] C. Lv, X. Zhou, L. Zhong, C. Yan, M. Srinivasan, Z. W. Seh, C. Liu, H. Pan, S. Li, Y. Wen, Q. Yan, *Adv. Mater.* **2021**, *34*, 1521.
[245] N. Yao, L. Yu, Z. H. Fu, X. Shen, T. Z. Hou, X. Liu, Y. C. Gao, R. Zhang, C. Z. Zhao, X. Chen, Q. Zhang, *Angew. Chem., Int. Ed.* **2023**, *62*, 1521.
[246] S. C. Kim, S. T. Oyakhire, C. Athanitis, J. Wang, Z. Zhang, W. Zhang, D. T. Boyle, M. S. Kim, Z. Yu, X. Gao, T. Sogade, E. Wu, J. Qin, Z. Bao, S. F. Bent, Y. Cui, *Proc. Natl. Acad. Sci. USA* **2023**, *120*, 2214357120.
[247] Y.-C. Gao, N. Yao, X. Chen, L. Yu, R. Zhang, Q. Zhang, *J. Am. Chem. Soc.* **2023**, *145*, 23764.

Nan Li is currently a Ph.D. student at the School of Materials Science and Engineering, Xi'an Jiaotong University. His current research interests include electrolyte design via molecular engineering and full-cell architecture design for rechargeable lithium metal batteries.

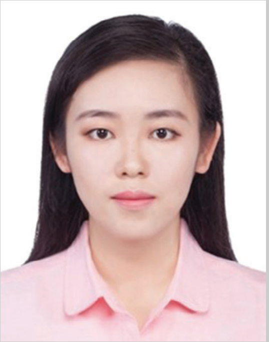

Xue Han is currently a Postdoctoral Researcher at the School of Materials Science and Engineering, Shanghai Jiao Tong University. She received her Ph.D. degree from the Beijing Institute of Technology in 2023. She has published more than 20 papers in peer-reviewed journals in energy storage materials. Her research interests include material synthesis, structure regulation, and design of electrode materials for supercapacitor and rechargeable aluminum batteries. Her current research interests focus on electrolyte design for lithium batteries.

Xinke Cui is currently a Ph.D. student at the School of Materials Science and Engineering, Xi'an Jiaotong University. His current research focuses on the design of new electrolytes for sodium-ion batteries.

Chaohe Xu is currently a Professor at the College of Materials Science and Engineering and National Engineering Research Center for Magnesium Alloys, Chongqing University. He received his Ph.D. degree in Materials Physics and Chemistry from the Shanghai Institute of Ceramics, Chinese Academy of Sciences, in 2012. From 2013 to 2015, he worked as a Postdoctoral Research Fellow at the National University of Singapore. Then, he moved to Chongqing University as an Assistant Professor from 2015 to 2021. He has published more than 120 papers in peer-reviewed journals and filled 17 patents for batteries. His current research interests include rechargeable magnesium batteries, all-solid-state batteries and their interface engineering.

Chong Mao is currently the Dean of Research Institute at Zhuhai Smoothway Electronic Co. Ltd (Smoothway), and responsible for R&D of advanced electrolyte for high-performance lithium/sodium ion batteries. He achieved his Ph.D. degree from Tsinghua University in 2016. He was selected as one of the top ten innovative young doctors and postdocs of Zhuhai in 2024.

Xiaobing Dai is currently the Chairman and Boss of Zhuhai Smoothway Electronic Materials Co., Ltd. She has been engaged in research on lithium-ion battery electrolytes for more than 20 years. She has led multiple research and development projects related to lithium-ion batteries and electrolytes and has applied for multiple patents.

Weijiang Xue is currently a Professor at the School of Materials Science and Engineering, Xi'an Jiaotong University. He received his Ph.D. degree from the School of Materials Science and Engineering, Tsinghua University in 2013. In 2014–2016 and 2016–2021, he worked as a Postdoctoral Researcher at Tsinghua University and Massachusetts Institute of Technology, respectively. Then, he moved to Xi'an Jiaotong University and has been a Professor since 2022. He has published more than 60 papers in peer-reviewed journals including two first-authored papers on *Nature Energy*. His current research interests include electrolyte design via molecular engineering and full-cell architecture design for rechargeable Li- and Na-based batteries.